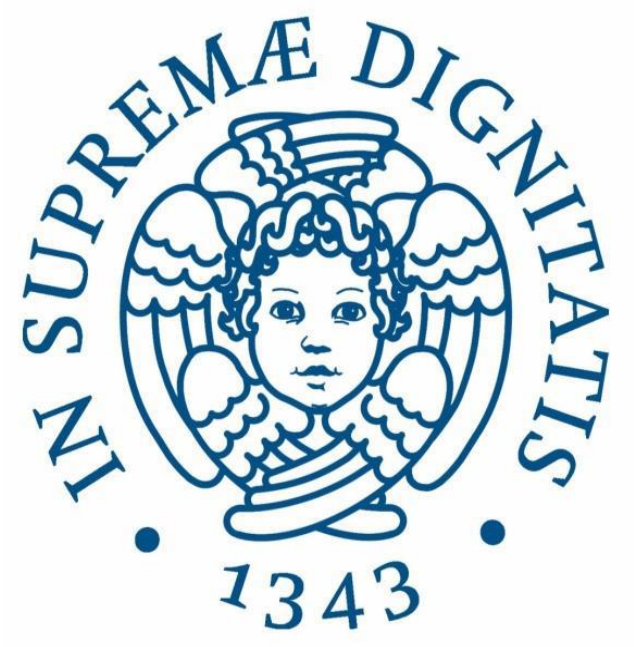

University of Pisa

Course of Molecular and Cellular Biology

Degree thesis

Characterization of the MAPT mutations Q336H and ΔK280 using a new intramolecular FRET biosensor

Candidate: Mariachiara Micaelli

Supervisor: Cristina Di Primio

Academic Year: 2015/2016

CONTENTS

ABSTRACT

Tau is a microtubule-associated protein mainly expressed in neurons, encoded by the MAPT gene. Mutations in the MAPT locus lead to abnormal accumulation of hyperphosphorylated tau in abundant intracellular inclusions known as neurofibrillary tangles (NFTs), a common feature of a group of neurodegenerative diseases known as Tauopathies.

In order to characterize the effect of ΔK280 and Q336H MAPT mutations FRET and FRAP techniques have been employed. To this aim the Conformational-Sensitive Tau Sensor (CST) that is based on the full length tau isoform 4R0N with the ECFP fused at the N-terminus and the EYFP at the C-terminus have been used. Since the CST allows to evaluate the changing in protein conformation and tau interactions with microtubules in living cells, two mutated CST constructs have been generated.

The study has revealed that Q336H and ΔK280 induced conformational changes in tau protein. In particular, Q336H alters the conformation by allowing the two ends of Tau protein to approach each other in a more closed loop-like structure. On the contrary, ΔK280 determined a conformational change by inducing a more relaxed three-dimensional structure and altered Tau stability on Microtubules by increasing the soluble Tau protein.

INTRODUCTION

1.Tauopathies

Alois Alzheimer (1907) firstly described the existence in brain of intracellular neurofibrillary tangles (NFTs) associated with extracellular plaques and only a few years later the presence of intracellular inclusions alone in different case of dementia. NFTs were first isolated from frozen autopsied AD brains. In 1963 Kid and Terry independently reported that they were made up of abnormal filaments alternating between 15 (at their narrowest point) and 30 nm (at their widest point) in width. Because it appeared that these filaments were wound in one another they were called paired helical filaments (PHF). They also found in NFT straight filament (SF), about 15nm wide. Years after, a protein of ~50kDa was isolated as the main constituent of PHF, but only in 1986 this protein was identified to be the Microtubule-Associated Protein Tau, and in 1988 the MAPT gene was cloned.

Tau is a microtubule-associated protein mainly expressed in neurons, encoded by the MAPT gene on chromosome 17q21-22. In a normal human brain are present six different isoforms, which differs mainly for the presence or absence of two inserts of about 29-58 aa in the N-terminal part, depending on the differential splicing of exons 2-3, and for the presence of three or four MTR at the C-terminal, depending on the differential splicing of exon 10. The differential splicing gives rise to three isoforms with three binding repeats (3R) or to four isoforms with four binding repeats (4R). The longest isoform of tau contains 80 sites of potential phosphorylation composed by serine and threonine residues, followed by a proline, almost all located in the regions flanking the microtubule binding repeats, as will be discussed further, and different tauopathies have shown to have different immunoreactivities to different tau phosphorylation epitopes, according to the immunohistochemistry analysis carried on fixed brain tissues.

Primary tauopathies are a heterogeneous group of neurodegenerative diseases that shares as a common feature the presence in neuronal and glial cells of deposits of misfolded, insoluble and hyperphosphorylated tau proteins. They are considered a subgroup of pathologies associated with Frontotemporal Lobar Degeneration (FTLD), a group of non-Alzheimer degenerative dementias with focal

cortical neuronal loss and gliosis, Frontotemporal Lobar Degeneration-Tau (FTLD-Tau) is their proper definition, used to differentiate them from other form of proteinopathies that fell under the FTLD spectrum. The age of onset is at 45-65 years, with a mean average in the 50s, with equal prevalence among men and women. Clinically they present the same variants displayed by FTLD, such as behavior, executive and language impairment associated with atrophy of the temporal and frontal lobe, giving rise to behavioral variant of FTD (bvFTD), semantic dementia (SD), and progressive non-fluent aphasia (PNFA), often associated with parkinsonism and motor neuron disease (MND). Patients with bv-FTD present dramatic changes in behavior and in personality, often displaying apathy and disinhibition, caused primarily by atrophy of the frontal cortex, with different region relating to different clinical phenotypes. Semantic Dementia is characterized by fluent anomic aphasia and behavioral changes, as a consequence of atrophy of the anterior temporal lobes, while Progressive non-fluent aphasia is characterized by a progressive disorder of speech and motor impairment, due to atrophy of the left frontal operculum.

FTLD-Tau can be sporadic or familial, the latter caused by mutations in the MAPT gene, with great clinical and pathological heterogeneity, mainly due to the different impact that these mutations can have on the physiological function of tau, which is to promote the assembly and the stabilization of the microtubules (MTs) required for morphogenesis and axonal transport. Genetic and environmental risk factors that could trigger tau pathology in sporadic forms of FTLD are still a matter of debate. The discovery of a polymorphic inversion along the MAPT coding region (Baker *et al.,* 1999) led to the definition of the H1/H2 haplotypes, in complete disequilibrium with each other, with the H1 including the noninverted sequence and the H2 comprising the inverted sequence and several other genes in its 900-kb length (Stefansson *et al.,* 2005). They differ in nucleotide sequence and in intron site, but they are identical at amino acid level. The more common H1 haplotype is significantly overrepresented in patients with Progressive Sopranuclear Palsy (PSP) and Corticobasal Degeneration (CBD) (Baker *et al*., 1999; Houlden *et al.,* 2001), while there is no difference between the H2 haplotype or the H2/H2 genotype observed in patients with Pick's Disease compared with control subjects (Morris *et*

al., 2002). Other studies also found an association between the H1 haplotype and the H1/H1 genotype with the development of sporadic FTD. One of the main region characterized by these polymorphisms is the promoter, altering the interaction with specific transcription factors and leading to tau expression deregulation. To further identify genetic variations contributing to the development of PSP, a GWAS study was carried out, and found significant signal associated with PSP risk in synthaxin 6 (STX6), eukaryotic translation initiation factor 2-α kinase 3 (EIF2AK3), and myelin-associated oligodendrocyte basic protein (MOBP) genes (Hoglinger *et al.*, 2011).

Hereditary forms of FTLD-Tau, which account for ~30% of FTD cases, are dependent on the presence of mutations in the MAPT locus, firstly associated with autosomal dominant inherited form of FTD with parkinsonism, leading to the definition of Frontotemporal Dementia with parkinsonism linked to chromosome 17 (FTDP-17). Familial cases with MAPT mutations present a wide range spectrum of pathology, starting typically from atrophy of frontal and temporal lobes, astrogliosis, swollen neurons and neuronal loss. Often cases are pathologically consistent with sporadic tauopathies and requires genetic testing to prove that are caused by mutations in the MAPT locus. Anyway tau inclusions in neurons and glia are hyperphosphorylated and acetylated in both familial and sporadic diseases, even if tau can undergo several post-translational modifications that can contribute to disease pathogenesis, as will be discussed further.

Finally, FTLD-Tau can be subdivided into several neuropathological diagnoses and classified based on the predominant tau isoforms that are present in the inclusion bodies. Because there is no involvement of the MAPT gene in the development of Alzheimer's disease, but other than the neurofibrillary tangles are also present senile plaques made of amyloid-beta protein, it is considered a “secondary tauopathy” belonging to the subgroup in which there is a balanced ratio of 3R and 4R tau isoforms in the inclusions.

Another feature that can help to discriminate between different tauopathies is the filament morphology, that have been studied in preparations of fixed tissues and dispersed filaments (Crowther et al., 2000). Tau filaments can be straight, ribbon-like or paired-helical. A recent study (Taniguchi-Watanabe et al., 2016) found out that the C-terminal (residues 243-406) band pattern of the pathological tau species

is distinct for each disease. Employing analysis of sarkosyl-insoluble tau banding patterns using antibodies against tau C-terminus, tauopathies can be classified in at least four types, Pick Disease, Progressive Supranuclear Palsy, Alzheimer's Disease, and Corticobasal Degeneration, even if it is also possible to extend this analysis to other tauopathies such Argyrophilic Grain Disease (AGD) and Globular Glial Tauopathy (GGT). They also discriminate that pathological 4R tau in MAPT intron mutation cases can be distinguishable from that in CBD and PSP cases by the analysis of the C-terminal fragments and the trypsin-resistant tau. A structurally distinct pathological tau protein seems to be involved in each disease and pathological proteins have the ability to convert normal tau into its own abnormal form. Indeed, the injection of brain homogenates from AD, PiD, CBD, PSP patients into Tg-mice overespressing 4R isoforms demonstrated that a similar pathology was induced (Clavaguera *et al*., 2013).

1.1 *Frontotemporal Dementia with Parkinsonism linked to chromosome 17*

Inherited forms of Frontotemporal Dementia were known from many years, but due to the clinic-pathological heterogeneity, the nomenclature has always been variable. The major clinical manifestations include cognitive impairment, behavioral disturbances, aphasia and parkinsonism. The discovery of mutations in the MAPT locus on the chromosome 17q21-22 led to the concept of Frontotemporal Dementia with Parkinsonism (FTDP-17) (Foster *et al*., 1997), which for a very long time it's also been used to name all of the pathologies that were found to be caused by mutations in that locus but that shown slightly different features, such as the inherited forms of Pick's disease; FTDP-17 also shows in its progression some features that are in common with Alzheimer's Disease, Progressive Supranuclear Palsy, Corticobasal Degeneration, but neuropathology and neuroimaging allow to discriminate different clinical phenotypes.

53 pathologic mutations have been reported in the MAPT locus (van der Zee *et al.,* 2014). FTDP-17 affects men and women equally, with the average age at onset being 49 years, with a range from the late 20s to the late 70s, similar to Frontotemporal Lobar Degeneration (FTLD). Its inheritance is autosomal dominant.

Differently from the other tauopathies, in FTDP-17 there isn't a prevalence of a tau isoform, mutations in the MAPT locus are heterogeneous and can cause the abnormal protein conformation or the disruption in 3R/4R ratio, or both, depending on the type of mutation.

The neuropathological phenotype associated with FTDP-17 MAPT vary substantially; the only invariable hallmark is the presence in neurons, or in both neurons and glia, of tau inclusions. Tau inclusions are abundant in cerebral cortex and white matter; subcortical and brain stem nuclei, as the spinal cord, are variably affected, but their anatomical distribution has been reported with different details in relation to individual mutations, even if the information is always obtained for the late stages of pathology. There may be mild atrophy of the caudate nucleus and a reduction in the pigmentation of the substantia nigra and the locus coeruleus. In advanced stages, the degree of atrophy varies and may be present throughout the frontal and temporal lobes, caudate nucleus, putamen, globus pallidus, amygdala, hippocampus and hypothalamus. Most often, the superior, middle, and inferior frontal gyri, as well as the superior, middle, and inferior temporal gyri, bear the brunt of the disease, with the anterior portion of the temporal lobe being particularly vulnerable. Brain atrophy may involve the frontal and temporal lobes asymmetrically.

As said before, the onset of FTDP-17 is insidious.Generally individuals shows three of the main cardinal symptoms, such as behavioral and personality disturbances, cognitive impairment and/or motor dysfunction. Clinical variability is seen in individuals with the same MAPT mutation, in different families or even within the same family. The behavioral and personality abnormalities include disinhibition, apathy, loss of empathy, aggressiveness, impulsive and/or compulsive behavior, lack of regard for personal hygiene, hyper orality including excessive use of alcohol and drugs. Progressive non fluent aphasia can be seen initially (Munoz *et al.,* 2007), and later progressive deterioration of memory, visual and spatial function, with development of a progressive dementia encompassing most cognitive domains that led the patient to completely lose the capacity of speaking. Parkinsonism associated with FTDP-17 MAPT is characterized by symmetrical bradykinesia, postural instability and rigidity affecting axial and appendicular musculatures,

absence of resting tremor, and poor or no responsiveness to levodopa. Even if no systematic work has been published on genotype-phenotype correlations in FTDP-17 MAPT, there is a general accordance that exonic mutations that do not affect the splicing of exon 10 are usually associated with a dementia-predominant phenotype. In contrast, intronic and exonic mutations that affects exon 10 splicing and lead to an overproduction of 4R tau isoform tend to be associated with a parkinsonism plus predominant phenotype (Ghetti *et al.*, 2015).

1.2 Pick's disease

Pick's Disease (PiD) is a progressive neurodegenerative disease that accounts for less than 5% dementia cases and usually occurs before 65 years of age. The most common clinical presentation is behavioral variant frontotemporal dementia, but language variants, both agrammatic and semantic types of primary progressive aphasia, have been reported. The diagnostic histological feature of Pick's disease are the Pick bodies, well-circumscribed, spherical, tau-immunoreactive and intracytoplasmic neuronal inclusions, which features the 3R tau isoform as the most prominent (Delacourte *et al.,* 1996). A small number of inclusions appear to contain 4R tau isoforms, as shown by IHC, and also to be thioflavine-S positive and to show immunoreactivity to acetylation-specific antibodies directed at K280 residue (Irwin *et al,* 2013). There are also swollen and achromatic “ballooned” neurons that are called Pick cells, prominent neuronal loss and astrocytosis. Pick bodies are found mostly in granule cells of the dentate gyrus, as well as the hippocampus and some cortical areas. Tau filaments are characterized by straight tubule of 15-18nm diameter and 22-24 nm diameter twisted filaments (Munoz *et al*., 1984). Pick Disease is usually sporadic, but discovery in mutations in the MAPT gene has contributed to the concept of hereditary forms of PiD, so it's also been associated with several clinical frontotemporal dementia (FTD) syndromes.

1.3 Progressive Supranuclear Palsy

Progressive Supranuclear Palsy is a 4R predominant tauopathy which shows atrophy of the subthalamic nucleus and brainstem tegmentum, and depigmentation of the substantia nigra. NFTs are present in the subthalamic nucleus, basal ganglia and brainstem, that are variably but characteristically associated with tufted astrocytes, and oligodendroglial coiled bodies. Tau filaments, as revealed by ultrastructural examination, are characterized as in PiD by straight tubule of 15-18 nm diameter and in NFTs by 14 nm diameter straight tubules (Arima, 2006; Dickson *et al.*, 2007). This typical PSP profile is also present in glial cells. Progressive supranuclear palsy (PSP) is the second most frequent cause of degenerative parkinsonism. In addition to parkinsonism, the clinical symptoms include early postural instability, supranuclear gaze palsy, and cognitive decline. It is typically a sporadic disorder with peak onset at age 63 and no reported cases before the age of 40.

1.4 Corticobasal Degeneration

Corticobasal Degeneration is another 4R tauopathy that shows as clinic-pathological feature asymmetrical atrophy in the posterior frontal and parietal lobes, with great neuronal loss in the substantia nigra. The minimal pathologic diagnostic features of CBD are cortical and striatal tau-positive neuronal and glial lesions, especially astrocytic plaques (Feany and Dickson, 1995). Small NFTs and corticobasal bodies can also be seen, and ultrastructural examination revealed that are made prevalently of 24 nm diameter twisted ribbons, but tubular structures and amorphous profile are seen in astrocytes, and twisted tubules in oligodendroglial cells (Arima, 2006). The age of onset of CBD is typically late adulthood, commonly set between the fifth to seventh decades of life. CBD, as PSP, is associated with a higher frequency of the MAPT H1 haplotype. The clinical presentation of CBD is a progressive asymmetric movement disorder with symptoms initially affecting one limb, including various combinations of akinesia and extreme rigidity, dystonia, focal myoclonus, ideomotor apraxia, and alien limb phenomena, with also a mild

cognitive impairment.

1.5 Argyrophilic Grain Disease

Argyrophilic Grain Disease (AGD) is a 4R tauopathy with grains positive to Gallyas staining (but not to all the silver impregnation methods) found mainly in dendrites and dendritic branches and some axons as the main hallmark of pathology (Tolnay and Clavaguera, 2004). Other non-specific lesions include: pre-tangle neurons, coiled bodies, tau-immunoreactive astrocytes, swollen neurons, NFTs and neuropil threads. Grains are small (4-8 nm diameter) round and spindle-shaped. Ultrastructurally, grains contain straight filaments of 10-20 nm diameter and tubular structures of 25 nm diameter.

1.6 Globular Glial Tauopathies

Globular Glial Tauopathies (GGT) are 4-repeat tauopathies characterized by tau-positive, globular glial inclusions, including both globular oligodendroglial inclusions and globular astrocytic inclusions. The brain shows atrophy of the frontal and temporal lobes. This is associated with argyrophilic (Gallyas) and 4R-tau oligodendroglial and non-argyrophilic 4R-tau immunoreactive globular astroglial inclusions, together termed globular glial inclusions, a feature that can help to discriminate GGT from PSP, with which shares a common astrocytic inclusions morphology (Ahmed *et al.,* 2013). Recently some mutations in the MAPT locus have been found to cause a pathologic phenotype typical of GGT, even if it shows to be prevalently sporadic (Tacik *et al.,* 2015). From a neuropathological point of view, it can be classified in different subtypes thanks to its wide pathological heterogeneity deriving from the different spread of the tau-positive inclusions, but if these subgroups fall under a pathological spectrum of the same disease entity or are to be considered distinct pathologies is still a matter of debate.

1.7 Alzheimer's Disease

Alzheimer's Disease (AD) is a chronic neurodegenerative disease with well-defined pathophysiological mechanisms, mostly affecting medial temporal lobe and associative neocortical structures. Neuritic plaques and NFTs represent the pathological hallmark of AD, and are respectively related to the accumulation of the amyloid-beta peptide (Aβ) in brain tissues, and to cytoskeletal changes that arise from the hyperphosphorylation of tau protein in neurons. According to the amyloid hypothesis of AD; the overproduction of Aβ is a consequence of the disruption of homeostatic processes that regulates the cleavage of the amyloid precursor protein (APP), a transmembrane integral glycoprotein of 110-130kDa. In the human brain there are different amyloid-beta species, but the most prevalent are the ones made of 40 and of 42 amino acids. This protein is metabolized by two distinct pathways, the secretory pathway (non amyloidogenic) and the amylodogenic pathway. The last is the one that give rise to the most toxic Aβ species, because APP is alternatively cleaved by β-secretase, releasing a smaller terminal N-fragment (sAPPβ) and a longer C-terminal fragment (C99) that contains the full amyloidogenic amino acid sequence. A further cleavage by γ-secretase yields the amyloid-beta peptides (Aβ), which are released as monomers that tend to aggregate progressively into dimers, trimers, oligomers, protofibrils and fibrils, to finally deposit and originate the amyloid plaques. Despite their similarities, $A\beta_{42}$ is more prone to aggregation and fibrillization. Aβ oligomers are considered the most toxic form of the amyloid derivates. They interact with neurons and glial cells leading to the activation of pro-inflammatory cascades, mitochondrial dysfunction and increased oxidative stress, impairment of intracellular signaling pathways and synaptic plasticity, increased tau phosphorylation and induction of neuronal apoptosis and cell death (Recuero *et al.*, 2004). These mechanisms altogether give rise to a self-perpetuating, positive feedback loop in which the production of Aβ peptides leads to deleterious events to the neuronal cells, which in turn leads to dysfunction of APP metabolism and more production of Aβ peptides.

As said before, the other neuropathological hallmark of AD is the presence of

intraneuronal lesions called neurofibrillary tangles. The main components of NFTs are the paired helicoidal filaments (PHFs) of 10 nm diameter with a helical period of 160nm, which are mainly constituted of hyperphosphorylated tau. Hyperphosphorylation of tau may be the initial step in the physiopathology of AD; other pathological events including abnormal APP cleavage may be secondary (Rhein and Eckert, 2007). Nevertheless, the lack of mutations in the MAPT gene associated to early or late onset AD weaken the hypothesis that tau pathology is the earliest event in AD (Oide et al., 2006). Therefore, other hypothesis regarding the initial steps of AD pathology have been proposed, involving the activity of proteins and enzymes that play their role upstream in the cascades involved in the regulation of the APP/Aβ and tau metabolism, such as GSK3β, which plays a pivotal role in the regulation of tau phosphorylation, leading to its hyperphosphorylation when over activated (Lovestone *et al.,* 1994).

Clinically, AD is defined by a gradual loss of memory and other cognitive functions, and the symptoms caused became more and more severe with the progression of the pathology. We can distinguish 4 stages: the preclinical stage, characterized by mild cognitive impairment, inability to plan and alteration in behavior; the mild dementia stage, characterized by learning impairment and spatial disorientation; the moderate dementia stage, with severe impairment of recent memory and language capacity; the severe dementia stage, in which almost all the cognitive functions are lost (Förstl *et al.*,1999).

Familial forms of AD have an incidence estimated from 5-10% to 50% and they are characterized by the presence of mutations and polymorphisms in some genes which encode for proteins implicated in early or in late onset of illness, like APP, ApoE, Presenilin 1 and 2, and many others whose inheriting rises the probability to develop AD (Karch *et al.*, 2014).

2. Tau

2.1 Gene and protein

A protein factor involved in microtubule assembly was firstly isolated from porcine brain in 1975 and named tau (Weingarten *et al.*, 1975). This protein was

recognized to be the same ~50 kDa microtubule-associated protein isolated from PHFs extracted from AD brains one year before, with the exception that the former was abnormally phosphorylated (Iqbal, 1974). Only in 1988 the MAPT gene encoding tau protein was cloned after the screening of cDNA libraries prepared from the frontal cortex of an AD patient (Goedert *et al.*, 1988).Six tau isoforms deriving from differential mRNA splicing were discovered to be characteristically expressed during human brain development (Goedert et al., 1989).The proteins varies from 352 to 441 amino acids in length, and they differ from each other for the presence or absence at the N-terminus of an insert of 29-amino or 58-amino acids, and for 31 amino-repeat at the C-terminus (fig.1).The latter depends on the differential splicing of exon 10, which give rise to three tau isoforms with four repeats (4R), or to three tau isoforms with three repeats (3R). The repeats with some adjoining sequences constitute the microtubule-binding domains of tau, each encoded by exon 9, 10, 11 and 12(Hutton *et al.*, 1998). The four motifs are copies of an 18 amino acids sequence that comprise a repeat, and each repeat is separated by a 13-14 amino acid inter repeat sequence (Lee *et al.*, 1988).

The human MAPT gene was discovered to be located on chromosome 17q21-22 (Donlon *et al.*, 1987), and is over 50kb in size, with two different haplotypes, H1 and H2, and contains 16 exons. The H2 haplotype differs from H1 by the deletion of a 238bp sequence upstream of tau exon 10. As said before, another feature of the H2 haplotype is the presence of an inverted sequence of 900kb. Compared with H2, the H1 haplotype is relatively heterogeneous. A total of 24 SNPs in the MAPT gene vary in the background of the H1 haplotype, and enables classification of the H1 into sub-variants that are sometimes associated with increasing risks of developing certain neurodegenerative diseases (Pittman *et al.,* 2004).

The transcription factors AP2 and SP1 bind to tau core promoter region upstream exon 1 and are necessary for promoter activity (Heicklen-Klein *et al.,* 2000; Gao *et al.*, 2005).

Tau protein has hydrophilic properties and exist normally as natively unfolded or intrinsically disordered protein (Jeganathan *et al.*,2008). The polypeptide chain of tau is highly flexible and mobile and has a low content in secondary structures. Tau protein contains three major domains: an acidic N-terminal part; a proline-rich

region and a basic C-terminal domain. Thus, tau protein is a dipole with two domains having opposite charge (Sergeant *et al.*,2008). This asymmetry is important for interactions between tau and microtubules and other partners as well for internal folding and aggregation.

The C-terminal portion binds to microtubules, promotes their assembly and is called “assembly domain” (Steiner *et al.*,1990).

The middle region of tau (150-240aa), termed “proline-rich domain” (Mandelkow et al., 2012) contains the PPXXP/PXXP motifs, which are targets of many proline-directed kinases and binding sites for proteins with SH3 domains, and the KKKK sequence involved in heparin binding (Avila *et al.*, 2004). The acidic part of tau does not bind to microtubules but project away from the microtubule surface and is termed “projection domain” (Hirokawa *et al.,* 1988). This domain may interact with other cytoskeletal elements, mitochondria or neuronal plasma membrane (Jung *et al.*, 1993; Brandt *et al.*, 1995; Al Bassam *et al.*, 2002).

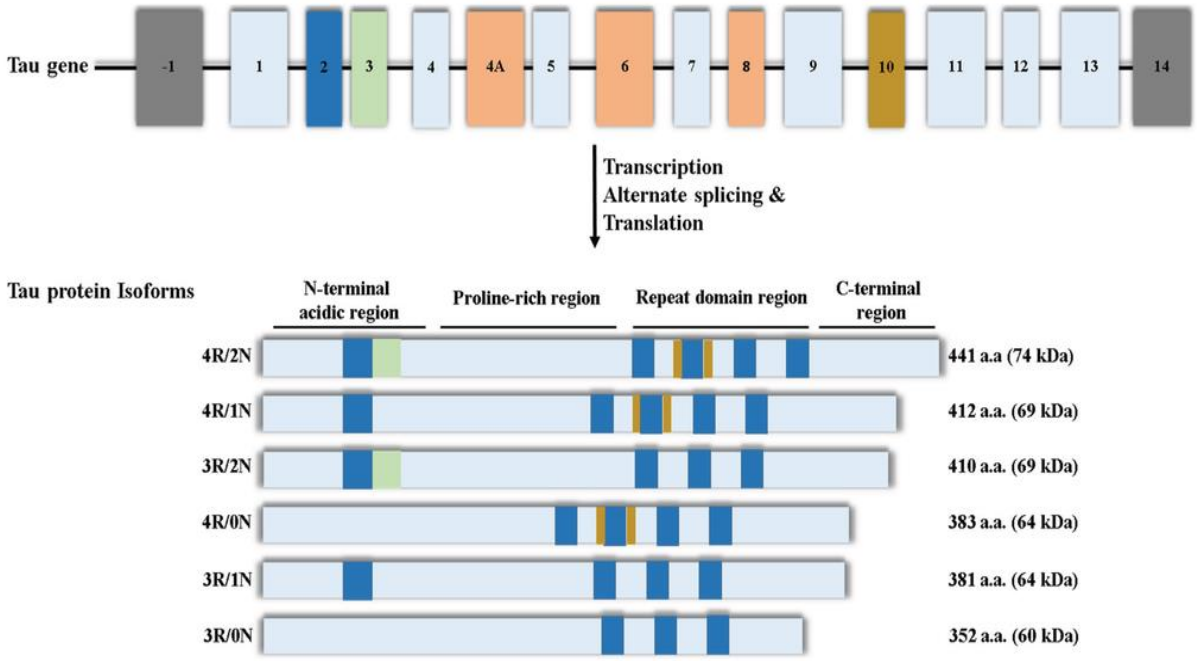

Fig. 1. MAPT gene and Tau splicing isoforms. The MAPT gene encodes for the tau protein. The protein includes 16 exons. The difference between the isoforms is given by the presence or absence of a 29 amino acids insert or of a 58 amino acids insert at the N-terminal, and by the number of repeats in the microtubule-binding domain, which vary between three and four.

(Image courtesy from Bukar Maina et al., (2016) “Nuclear Tau and its potential role in Alzheimer's disease” *Biomolecules, 6*(1),9)

2.2 Physiological role

Tau is a multifunctional protein, with numerous binding partners. Its main function is to bind and stabilize microtubule (MT), as was firstly observed (Weingarten *et al.,* 1975), thus it is considered to be a microtubule associated protein (MAP). The regulation of microtubule dynamic instability is due to its capability in regulating tubulin polymerization (Trinczek *et al.,* 1995). The tubulin binding site is located at the C-terminal of tau, which is highly acidic, and can be regulated by tau post translational modifications, such as phosphorylation. Phosphorylation may alter the protein positive charge thus leading to a change in conformation and in

detachment from microtubules (Fisher *et al.,* 2009). Tau may interact with microtubules directly or indirectly. Direct interaction includes the binding, stabilization and assembly. NMR analysis detect specific sequences involved in MT binding (Mukrash *et al.,* 2007). These sequences include ^{240}KSRLQTAPV^{248,} ^{275}VQINKKLDLS^{285}, and ^{297}IKHV^{300}, the latter both coded by exon 10, and this can explain why the 4R isoforms binds more strongly to microtubules than the 3R isoforms (Panda *et al.,* 2003).

Binding of tau to microtubules can take part in axonal transport and can interfere with binding of motor proteins. A gradient of tau along the axon with the highest level around the synapse might facilitate the detachment of motor proteins from their cargo near the presynaptic terminal and might increase axonal transport efficiency (Dixit *et al.,* 2008).

Tau can also bind spectrin and actin filaments (He et al., 2009), and this might allow tau-stabilized microtubules to interconnect with neurofilaments that restrict the flexibility of the microtubule (Kolarova *et al.*, 2012).

Tau can also act as a postsynaptic scaffolding protein. As a scaffold protein, tau modulates the activity of Src tyrosine kinases, c-Src and Fyn, and facilitates c-Src-mediated actin rearrangements (Sharma *et al.,* 2007). In the case of Fyn, it has been suggested that tau normally tethers Fyn to PSD-95/NMDA receptor signaling complex (Ittner *et al.*, 2010). Tau can also act as a scaffold protein in oligodendrocytes, where it my connect Fyn and microtubules in order to enable processes extension (Klein *et al.,* 2002).

Another function of tau is involvement in growth factor signaling (Niewiadomska *et al.,* 2005; Niewiadomska *et al.,* 2006). Under NGF stimulation, tau is distributed at the ends of cellular extensions, where it associates with actin in a microtubule-independent manner (Yu *et al.,* 2006). Tau facilitates signaling through receptors for NGF and EGF, that may increase the activity of the mitogen-activated protein kinase (MAPK).

2.3 Post translational modifications

Several modifications have been described for tau protein. It is subjected to modifications by serine, threonine and tyrosine phosphorylation, isomerization, glycation, nitration, O-GlcNAcylation, acetylation, oxidation, polyamination, sumoylation, ubiquitination, and proteolytic cleavage (truncation).

Phosphorylation

Phosphorylation is the main post-translational modifications affecting tau that it's been described. Almost 85 phosphorylation sites have been identified in tau molecule. Kinases that are involved in tau phosphorylation can be divided into three classes: proline directed protein kinases (PDPK), non-PDPK protein kinases and tyrosine protein kinases (TPK).

- GSK-3

Glycogen synthase-3 (GSK-3), belongs to the PDPK class, and is a serine/threonine-specific kinase whose activity is regulated by phosphorylation. 42 GSK-3 phosphorylatable sites on tau have been identified. The level of GSK-3 increase in neurodegeneration (Pei *et al.*, 1997), and its activity correlates with the increasing amount of NFTs (Leroy *et al.,* 1992), where it is found (Yamaguchi et al., 1996). The GSK-3β isoform preferentially phosphorylates Ser/Thr residues followed by a proline (Ser/Thr-prolin motif). The most favorable phosphorylation sites of GSK-3β are Ser396/Ser404 in the C region of tau (Liu *et al.,* 2006). It is also been observed that tau phosphorylation by GSK-3β only at the C-region increased its activity of stimulating MT assembly (Liu et al., 2007). GSK-3β also phosphorylates tau at Thr231, one of the most prominent sites for the regulation of its activity at early stages. The modification at this epitope causes a conformational change in the protein affecting its ability to bind to MTs, and it is considered to be an early event in the progression of AD (Daly *et al.,* 2000).

- Cdk5

Cyclin-dependent kinase 5 (cdk5) is a serine/threonine kinase which belongs to the

PDPK class. Its activity is regulated by phosphorylation, and by the binding of an activator subunit, p35 or p25 which is generated by calpain-dependent proteolytic cleavage of p35 (Lee *et al.,* 2000). The p25/cdk5 holoenzyme phosphorylates tau and reduces its ability to bind to microtubules, it alters cell morphology, causes cytoskeletal disruption and apoptotic cell death (Patrick *et al.*, 1999). It phosphorylates tau on Ser202, Ser205, Thr212, Thr217, Thr235, Ser396 and Ser404, as it appears in AD brains.

- CK1

Casein Kinase 1 (CK1) is a family of protein kinase non-PDPK. It can phosphorylate tau at Ser202/205 and Ser396/404 *in vitro* and in cell culture, modulating its binding affinity for microtubules (Li *et al.*, 2004).

- Dyrk1A

Dyrk1A, a non-PDPK kinase, phosphorylates tau mainly at Thr181, Ser199, Ser202, Ser205, Thr212, Thr217, Thr231, Ser396, Ser400, Ser404 and Ser422, all Ser/Thr phosphorylation epitopes belonging to the P region. Phosphorylation by Dyrk1A inhibits tau capability of microtubule assembly and increases its ability to self-aggregate (Ferrer *et al.,* 2005).

- PKA

Cyclic AMP (cAMP)-dependent protein kinase (PKA) is a serine/threonine protein kinase which belongs to the non-PDPK class. PKA catalyzes tau phosphorylation and triggers the kinase activity of GSK-3β at several AD-relevant phosphorylation sites, including Ser214, Ser262 and Ser409, which span over the P-region, the MT binding repeats and the C-region of tau, decreasing MT assembly (Liu *et al.,* 2007).

- CaMKII

CaMKII regulates important neuronal functions including neurotransmitter synthesis and release, modulation of ion channel activity, synaptic plasticity and gene expression. It phosphorylates tau at Ser262, Ser356, Ser409 and Ser416, and these sites are phosphorylated in brains of AD patients (Steiner *et al.,* 1990).

- Phosphatases

Protein phosphatases (PPs) responsible for dephosphorylation of tau include: PP2B, PP2A, PP1 and PP5. PP2B is one of the main serine/threonine phosphatases in the brain; its activity depends on Ca^{2+}/calmodulin, and is associated with microfilaments and MTs development. PP2A is localized on MTs and binds tau directly. PP5 is associated with MTs and dephosphorylates tau in neuronal cytoplasm. The inhibition or the absence of this phosphatase in the cells causes the hyperphosphorylation of tau protein suggesting a possible role of this protein in AD development (Pevalova *et al.,* 2006).

- Critical phosphorylation sites

Many epitopes can be considered involved in tau aberrant activity in AD and in other tauopathies. AT8 epitope (Ser199/Ser202/Ser205) is considered an early hallmark of AD and other tauopathies. The hyperphosphorylation of these three residues can cause MTs instability, diminished mitochondria axonal transport and neuronal cell death (Alonso *et al.,* 2010; Shahpasand *et al.,* 2012). The same effect is due to the hyperphosphorylation of residues Thr212/Thr231/Thr262.Kinetic studies also confirmed that the AT8 epitope, Thr212, Thr231/Thr235, Ser262/Ser356, and Ser422 are among the critical phosphorylation sites that convert tau into pathological molecule prone to aggregation. Phosphorylation at Ser262/Ser356 its also been reported to inhibit MTs assembly (Biernat *et al.,* 1993; 1999). Phosphorylation of Ser396/Ser404 by GSK-3β increases tau activity of stimulating MTs assembly (Liu et al., 2007).

Pseudo phosphorylation of Ser422 has shown an increase in aggregation and a reduced cleavage at Asp421 (Guillozert-Bongarts *et al.,* 2006).

Glycosylation

Glycosylation is the attachment of oligosaccharides to a protein. There are two types of glycosylation: N-glycosylation and O-glycosylation. The first derives from the attachment of a sugar on the amine radical of asparagine, while the second from the attachment of a sugar on the hydroxyl radical of serine or threonine. Protein tau can be O-GlcNAcylated *in vitro* in recombinant systems and in some

transfected cell-lines in culture (Smett-Nocca *et al.,* 2011). *In vivo* it has been shown to reduce tau phosphorylation in rat cortex and hippocampus (Yuzwa *et al.,* 2008).

Glycation

Tau glycation seems to prevent its degradation and to promote its accumulation (Edesma *et al.,* 1996). It triggers the production of free radicals amplifying oxidative stress, which in turn increases tau phosphorylation (Su *et al.,* 2010). By this mechanism, tau can be oxidized at C322, leading to PHF assembly (Landino *et al.,* 2004). Oxidative stress promotes tau nitration which indicates that tau glycation can indirectly induce both tau oxidation and nitration, leading to tau phosphorylation and oligomerization (Zhang et al., 2006).

Acetylation

After phosphorylation, acetylation is one of the major post-translational modification to which tau undergoes. Lysine acetylation in particular it is been observed to neutralize charges in the MT binding domain interfering with tau capability to bind MTs. Acetylation of Lys280 increases cytosolic tau fraction and it's correlated with tau hyperphosphorylation. Acetylated Lys280 is present in intracellular NFTs and it precedes tau truncation (Cohen *et al.,* 2011; Irwin *et al.,* 2012).

Polyamination

The reaction of polyamination by transglutaminase (TGs) involves a glutamine (Q) as acyl donor and a lysine (K) as acyl acceptor. Eight acceptor sites and ten donor sites were identified on tau protein (Murthy et al., 2008). Polyamination is observed on the protein before NFTs formation (Singer et al., 2002).

Ubiquitination

Tau has been shown in non-pathological conditions to be ubiquitinated and proteolytically processed by UPS (Ubiquitin-proteasome-system) (Liu et al., 2009). Tau ubiquitination can occur in PHFs after its hyperphosphorylation and

glycosylation, and increases as PHFs maturate (Bancher et al., 1991; Iqbal et al., 1998).

Nitration

Nitration is the addiction of nitrogen dioxide on tyrosine of an organic molecule. It occurs at 4 sites, and it is been suggested to be involved in tau aggregation (Horiguchi et al., 2003). Nitration was also proposed to impair tau ability to promote tubulin assembly (Reynolds et al., 2006), leading to tau oligomerization (Zhang et al., 2005).

2.4 Tau cleavage

Tau protein truncation occurs in AD brains at D421, E391, D13 residues, and enhances the capability of the protein to aggregate and cause neuronal apoptosis (Chung *et al.,* 2001). These truncated forms are especially found in PHFs (Mena et al., 1996), and this suggest that they can contribute to protein aggregation in AD. Tau phosphorylation at Ser422 seems to protect tau from being cleaved at Asp421 by caspase-3, hence dephosphorylation of this epitope is required for its proteolytic processing (Guillozet-Bongaarts *et al.,* 2007).

Tau cleavage can be achieved by calpains, and especially calpain-2 that co-localize with tau filaments in AD and in frontotemporal dementia (Adamec *et al.,* 2002, Corset *et al.,* 2008).

2.5 Tau aggregation

Tau aggregates display different morphologies in different tauopathies. The type of aggregate formed is determined by the tau isoform involved or in the mutations in the MAPT gene (Crowther *et al.,* 2000). Tau appears to be highly phosphorylated and is more susceptible to aggregate than non-phosphorylated tau (Avila *et al.,* 2004). The increased pool of soluble tau undergoes others conformational changes which may support initial steps of tau assembly into filaments (Hyman *et al.,* 2010). Physiological and pathological tau species include: monomers, dimers/trimers,

small soluble oligomers, insoluble granular tau oligomers, filaments, pretangles, large non-fibrillary tau aggregates, neurofibrillary tangles and ghost tangles (Cowan *et al.,* 2013; Brunden *et al.,* 2008). Tau oligomers are considered the most toxic among the tau species, and that fibrillary tau is considered neither necessary nor sufficient for tau-induced toxicity, and may even represent a neuroprotective strategy (Spires-Jones *et al.,* 2011). According to some studies, the first abnormal event in AD is the formation of the PHF-tau minimal core unit comprising tau truncated at Glu-391. A series of phosphorylation events along the N-terminal (Luna-Munoz *et al.,* 2007; Mena and Luna-Munoz, 2009) would favor the action of caspase-3 that cleaves tau at Asp421 (Gamblin *et al.,* 2003). This cause a sequential cycles of events in which truncated tau captures full length tau, which undergoes a cleavage and became able to bind further full length molecules with increased avidity (Wischik et al., 1996) generating oligomeric aggregates that can develop to neurofibrillary tangles (fig.2).

Tau has long stretches of positively and negatively charged region which don't allow intermolecular hydrophobic association. Two hexapeptides, ^{275}VQJINK^{280} and ^{306}VQJVYK^{311} which are respectively located at the beginning of the second and third MBDs are prominent in generating β-sheets structures during tau aggregation process (Von Bergen *et al.,* 2000; Fisher *et al.,* 2009). Self-aggregation is inhibited by the presence of intact N- and C-terminal domains, but when these ones are aberrantly phosphorylated or cleaved, the conformational structure changes exposing the sticky repeat regions which leads to the formation of PHFs (Alonso *et al.,* 2001).

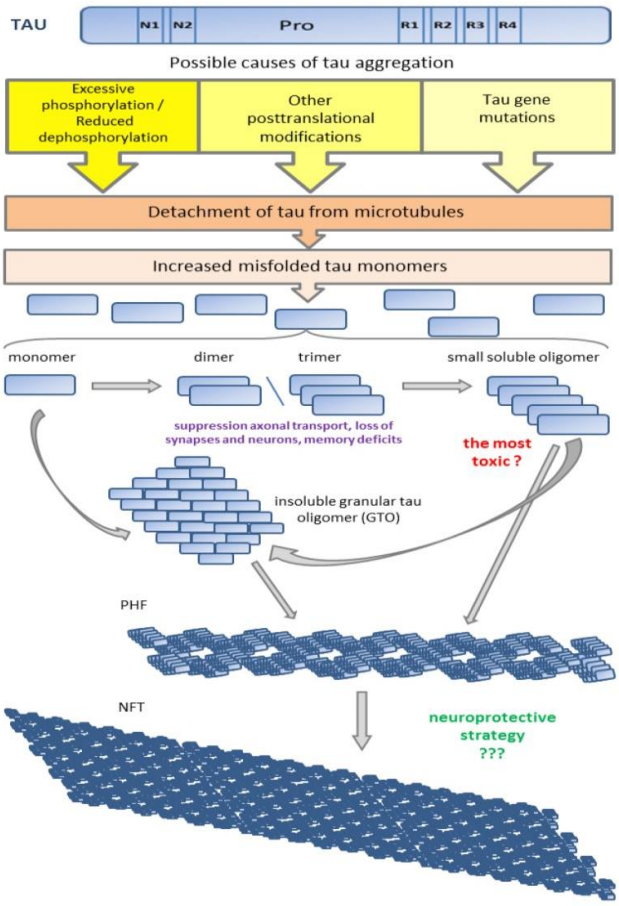

Fig 2. Sequence of stages leading to tau aggregation in NFTs. Detachment of tau from microtubules increases amount of misfolded tau monomers. Monomers aggregate into small soluble tau oligomers (GTOs). Probably both, small oligomers and GTOs form paired-helical filaments (PHFs) but GTOs are considered to be the main precursor of PHFs. Subsequently PHFs spontaneously aggregate into neurofibrillary tangles (NFTs).

(Image courtesy from Mietelska-Porowska et al., 2014 “Tau protein Modifications and Interactions: Their role in function and dysfunction” *Int.J.Mol.Sci. 15).*

2.6 Secretion

Tau can be directly involved in the spreading of AD and other tauopathies to neighboring neurons. Tau pathology can be induced and propagated by the injection of tau oligomers into wild type or mutated MAPT transgenic mice (Iba et al., 2013) and exogenous tau aggregates can be transferred from cell to cell *in vitro* (Iba *et al.,* 2013; Frost *et al.,* 2009) and *in vivo* (De Calignon *et al.,* 2012 ; Liu *et al.,* 2012). In the case of soluble monomeric or oligomeric tau, the exocytosis

appeared to be clathrin-dependent (Rubinzstein *et al.,* 2006), while other tau aggregates could bind heparin in the extracellular matrix and be internalized by macropinocytosis (Holmes *et al.,* 2014). It is also been observed that tau spreading could follow a non-conventional secretory pathway led by the RER and Golgi. COPII vesicles budding from the ER containing tau at their surface can fuse directly with the plasma membrane for secretion (Nickel *et al.,* 2009). Another hypothesis is that tau secretion could occur through non-COPII-coated vesicles forming at the ER or vesicles forming at the Golgi with tau attached to surface (Ponnanbalam *et al.,* 2003). Another study reported that hyperphosphorylation and cleavage at Asp421 increased tau secretion, at least in Hela cells (Plouffe *et al.,* 2012), starting a vicious cycle that led to the amplification of secretion. Hyperphosphorylation would enhance the secretion trough microvesicles or the other non-conventional pathways mentioned before. Dephosphorylation would occur in the extracellular space and dephosphorylated tau would activate the muscarinic receptors, inducing an increase of intracellular calcium, an event linked to the increase of tau hyperphosphorylation.

2.7 Mutations

53 MAPT mutations have been identified, and they can be classified on the basis of their position on the gene. Mutations affect tau at mRNA splicing level and at protein level. The majority of mutations affect the coding region, comprising missense mutations, silent mutations and deletions. Many mutations are located close to the splice-donor site of the introns downstream exon 9 and 10. Most coding region mutations are located in the MT-binding region (exons 9-12) of tau or close to it (exon 13). Mutations affecting exon 1, 9, 12 and 13 affect all tau isoforms, while mutations in exon 10 affect only 4R isoforms. The primary effect of intronic mutations and of some mutations affecting splicing regulatory elements is exerted at the level of RNA splicing, thus leading to altered expression of tau isoforms, in particular altering the ratio between the 3R and the 4R isoforms in the case of mutations affecting exon 10. Mutations can also be classified on the basis

of their molecular effect on tau-MTs interaction and/or fibril formation. Some mutations however share the same effects (Hutton *et al.,* 1998; Spillantini *et al.,* 1998).

Mutations altering the tau-MTs interaction and fibril formation

Being located in the MBD, most missense mutations can cause an alteration in the binding of tau protein to MTs. Most of these mutations are located in exon 9, 11, 12 and 13, with the exception of P301L and P301S which are in exon 10 and share the same feature and, excepting Q336R/H, located in exon 12 that is been observed to enhance tau binding affinity to MTs, as will be discussed further. Also some mutations located outside the MBD can have an effect on binding affinity, as it is has been observed for mutations located on exon 1. Other mutations can have pre-fibrillogenic effects, as it has been observed *in vitro* on heparin-induced tau filament assembly (Goedert *et al.,* 1996).

Mutations altering tau RNA splicing

All intronic mutations and a few coding-region mutations affect the splicing of exon 10 altering the ratio between the 4R and the 3R isoforms, in most cases increasing the 4R isoform. The majority of intronic mutations are located in the intron following exon 10, with only two mutations described in the intron following exon 9. Missense mutations affecting splicing of exon 10 are N279K, G303V and S305N, and silent mutations are L284L, N296N and S305S (Gasparini *et al.*, 2007).

Mutations altering Tau-MTs interaction, fibril formation and RNA splicing

Several missense mutations exert their effects at both protein and RNA levels. ΔK280, ΔN296 and N296H mutations greatly reduce the ability of tau to bind to MTs and to promote MTs assembly *in vitro*. The opposite effect it has been observed for Q336R/H and S305N mutations. Effects at the mRNA level also have been demonstrated for these mutations, and they increase the splicing-in of exon

10, while others leave it unaltered and the ΔK280 decreases it.

3. Q336H and ΔK280

3.1 Q336H

Q336H is a missense mutation located in the coding region of exon 12. It has been observed in one patient with an inherited form of dementia with features typical of Pick disease. This patient shared a common patho-mechanism with a previously reported case variant affecting the same codon, Q336R (Pickering-Brown *et al.,* 2004). Sarkosyl-insoluble tau isoforms extracted from samples of brain tissue displayed a high prevalence of 3R isoforms, as expected from a Pick Disease phenotype. Study *in vitro* on the effect of the mutation on tubulin polymerization found out that Q336H in the 3R0N tau isoform promoted MTs polymerization at a rate greater than in the WT 3R0N tau. The same result was obtained about the promotion of tau filament formation, infact Q336H highly promotes tau polymerization more in the 3R isoform rather than the 4R isoform (Tacik *et al.,* 2015).

3.2 ΔK280

This is a coding mutation affecting exon 10 only in 4R tau isoforms, because it is in the exon 10 “linker region” between two microtubule binding repeats, which isn't present in the 3R isoforms, and which contains the following amino acids, ^{274}KVQIINKKLD^{287}. The deletion removes either the second or the last lysine residue at position 280 or 281, and by the use of microtubule assembly assays it has been shown that the mutation induced a strong decrease in microtubule binding affinity than the wild type protein (Goode and Feinstein 1994; Trinczek *et al.,* 1995). It is a mutation that affects transcript tau and tau protein, affecting splicing of exon 10 inhibiting its inclusion, and diminishing tau ability to promote microtubule assembly *in vitro* (Rizzu *et al.,* 1999). A study conducted on cell culture has shown that ΔK280 decreased the ability of tau to regulate the percentage of

time microtubule spent growing, shortening and attenuated, showing a massive effect on the regulation of the growth rate compared to 4R wild type tau, while not altering the effect on the shortening rate (Bunker *et al.,* 2006). It is also been observed that ΔK280 strongly promotes the aggregation of tau into paired-helical filaments (PHFs), because it enhanced the propensity of the protein to form β-structure (Barghorn *et al.,* 2000).

Various transgenic mouse models have been developed during the years. One of the most significant expressed the transgene with the full length tau 4R2N under the control of a TET-OFF system, and it has been observed that tangles started at 24 months of age, although it was also present a great pre-tangle pathology, including hyperphosphorylation at specific epitopes (262, 356), and conformational changes that enhance the propensity to aggregate (Eckerman *et al.,* 2007). Another mouse model used as transgene a fragment from 244 to 272, comprising the four microtubule binding domains. In this model tangles formation started early from 2-3 months of age, with great neuronal loss in the hippocampus (Mocanu *et al.,* 2008).

4. FRET and FRAP

4.1 FRET

Fluorescence resonance energy transfer (FRET) is a mechanism of energy transfer between two light sensitive molecules. An excited fluorophore can deactivate by non-radiative transfer of energy from the excited dipole of the donor fluorophore to the dipole of the accepted one. The acceptor fluorophore in turn can return to its ground state by different mechanisms including photon emission, non-radiative dissipation or again energy transfer to another acceptor molecule. In order for FRET to occur, there is the necessity to have an overlap of the emission spectrum of the donor and the excitation spectrum of the acceptor. The second requirement is a close proximity of donor and acceptor, ranging in a distance of 1-10nm. In addition to a sufficient proximity of the chromophores, an appropriate relative orientation of the dipole vectors is necessary for a high FRET to occur.

Many biological processes like protein interactions take place within the spatial range at which FRET occurs, so it is been widely used as a tool to study molecular interactions. The efficiency of FRET is given by the ratio of donor excitation events that result in FRET, to the total number of excitation events, and is directly related to the distance R between the fluorophores by the power of six: $E= R_0^6/R^6+ R_0^6$. While R describes the actual distance between fluorophores, R_0 is called the Förster distance and describes the distance at which E is 0.5, or where exactly 50% of the donor excitation events lead to FRET: $R_0=0.2108[k^2\Phi_0 n^{-4}J]^{1/6}$. R_0 is different for each FRET pair, and is used as a parameter to describe the capabilities of this pair to produce FRET under certain conditions, so it is used as a criteria to select FRET pairs. Because FRET efficiency and distance of donor and acceptor are relatable, FRET has found many applications in the last decades, often to prove the interaction and the co-localization of two probes, which are bound to fluorophores. An important discovery in relation to FRET was the description of the Green Fluorescent Protein (GFP) in 1962 by Osamu Shimomura (Shimomura, 2009). GFP is a naturally fluorescent protein of the jellyfish species *Aequorea victoria*. After the elucidation of its DNA coding sequence and the possibility to express it outside *Aequorea victoria,* synthetic variants of the protein have been produced, obtaining different fluorophores that shifted the color emission to other wavelengths, thereby producing fluorescent proteins that span the entire visible spectrum from blue to red and even beyond (Olenyc *et al.*, 2007). The major consequences of this discovery is the possibility to develop many donor-acceptor pairs, and to genetically link them to a variety of spacers leading to intramolecular FRET. If a spacer in some way responds to a change in the environment, leading to an alteration in the distance between the fluorophores this will result in a change of the FRET signal. This kind of construct is a FRET-biosensor, and since an unlimited variety of spacers can be designed and associated with a great diversity of fluorophores pairs, it is possible to use these biosensors for studying a lot of biological processes, and make them quantitatively measurable and visible. For example, it is been used in different studies of Alzheimer's disease, like the sensor constructed to detect Aβ oligomers using CFP and YFP respectively as donor and acceptor (Takahashi *et al.*, 2012). Other

studies utilized FRET to detect the interaction between tau and MTs (Nouar *et al.,* 2013).

Methods to measure FRET efficiency

FRET efficiency is measured and used to identify interactions between the labeled complexes. There are several ways to measure FRET efficiency, by monitoring the changes in the fluorescence emitted by the donor or the acceptor, but the two mainly used are Sensitized Emission and Acceptor Photobleaching.

Sensitized Emission

This method measures the variation in the acceptor emission intensity (Clegg and Robert, 2009). When donor and acceptor are in proximity (<50Å) due to interactions of the two molecules, the acceptor emission will increase due to the intermolecular FRET from the donor to the acceptor. This method is preferentially used to monitor protein conformational changes, labelling the protein with a donor and an acceptor at two loci. When a modification of the protein conformation changes the donor and the acceptor distance and relative orientation, FRET change is observed.

Acceptor Photobleaching

FRET efficiency can also be inferred from the photobleaching rates of the donor in the presence or absence of an acceptor (Clegg and Robert, 2009). This method is based on the excitation of the single donor in specimen with or without the acceptor fluorophore and the monitoring of the donor fluorescence over time. Photobleaching consists in the permanent inactivation of excited fluorophores, so resonance energy transfer from and excited donor to an acceptor fluorophore prevents the photobleaching of that donor fluorophore, so a high FRET efficiency consist in a longer photobleaching decay time constant.

4.2 FRAP

Fluorescence photobleaching after recovery (FRAP), is a technique commonly used

to study the dynamics of fluorescent molecules in living cells (Cardullo et al.,1991; Mullineaux and Kirchoff 2007; Carisey et al., 2011). The technique now is routinely used to monitor qualitatively and quantitatively the dynamics of molecule both on cell surface and within the cytoplasm. FRAP is been used to measure the rate and extent of molecular mobility, the presence of binding interactions, and how these properties are affected with different treatments. These kinetics data are then quantified by analyzing the resulting fluorescence-intensity recovery curve versus time (Waters, 2007). As described previously, fluorescent molecules are generally susceptible to photobleaching, which result in the signal fading over time. Photobleaching is dramatically accelerated as the excitation light intensity increases; in the presence of an intense laser source, complete photobleaching can occur in the order of milliseconds. FRAP takes advantage of the rapid and irreversible photobleaching of fluorescently labeled molecules within a region of interest using a laser tuned to an appropriate wavelength for short duration of time (typically less than 20 msec). Following the light pulse, the fluorescence intensity is monitored in an area around and including the region of interest using a low-intensity light source to monitor the movement of photobleached and fluorescent molecules over time. FRAP has two quantitative parameters: the mobile fraction (M_{ob}), which is the amount of fluorescence recovered after photobleaching, and the recovery half time ($t_{1/2}$), which is the minimum time required for the recovery of 50% of the fluorescence in the region of irradiation (ROI):$t_{1/2}$ is inversely proportional to the diffusion coefficient of the fluorescent molecule which is in turn influenced by the dimension of the molecule and binding interactions. FRAP analyses allow to plot a recovery curve reflecting diffusion and binding dynamics. These recovery curves can be fitted by two different equations: a FRAP curve fitted by a simple exponential equation, representing the case in which diffusion and binding cannot be separated; a FRAP curve fitted by the sum of the two exponentials where there is an initial short diffusive phase followed by a longer binding phase (Nouar *et al.,* 2013). FRAP techniques is often used to obtain information about the mobility of proteins and about protein interactions that can influence the diffusion of molecules. In recent reports tau mobility has also been studied by FRAP, and the results showed that the FRAP curve is fitted by two exponentials, suggesting the presence

of a diffusive phase and a binding one (Nouar *et al.,* 2013). The recovery curve can change in times of recovery or in the kind of fitting if conditions in the cell changes for example stabilizing or destabilizing MTs (Breuzard *et al.,* 2013; Nouar *et al.,* 2013).

MATERIAL AND METHODS

1.Site-directed mutagenesis

The CST construct used, already present in the lab, comprise Tau-D, a 4R isoform which lacks of the N-terminal domains and has 383aa, CFP and YFP genes inserted respectively upstream and downstream the TAU gene, which sequence is separated from the fluorophores by a linker sequence coding the peptide RSIVT. The promoter for the expression of the construct is the CMV, a ubiquitous promoter that determines a high expression of the protein in several cell types. This CST has been mutagenized in single residues. The mutations induced are the Q336H missense mutation and the deletion ΔK280 (fig.1). To modify the residues of interest the Site-Directed Mutagenesis Kit Q5 (New England BioLabs) was used.
The primers used to mutagenized the sequence of TAU were:
Fwd 5'-AGGAGGTGGC**CAC**GTGGAAGT-3' for Q336H;
Rev 5'-GGTTTATGATGGA**TGT**TGCC-3' for Q336H;
Fwd 5'-AAGCTGGATCTTAGCAAC-3' for ΔK280;
Rev 5'-ATTAATTATCTGCACCTTCC-3' for ΔK280.

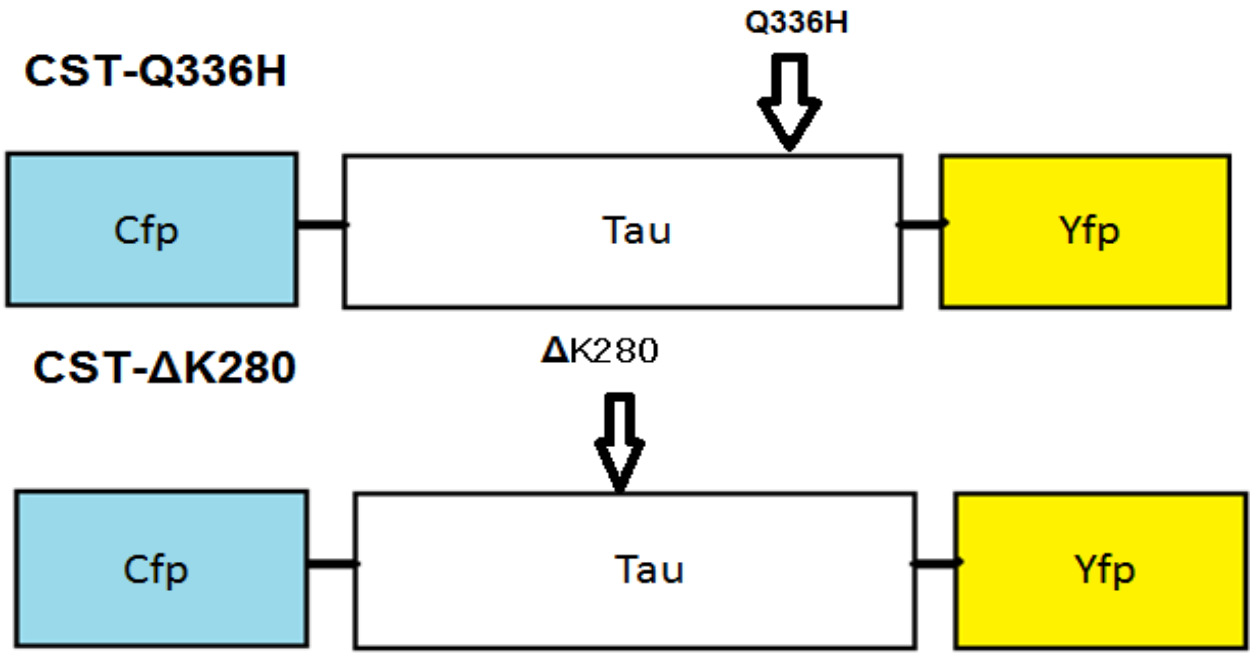

Figure 1. Mutagenized CST. The image reports the sites mutagenized of the tau sensor.

2.Cell cultures and transfection

HeLa and immortalized hippocampal neurons HT22 cells were routinely cultured in Dulbecco‘s Modified Eagle‘s Medium (DMEM) low glucose (Euroclone), supplemented with 10% Fetal Bovine Serum (FBS), 100 U/ml Penicillin and 100 µg/ml Streptomycin.

Cells were plated at 60%-70% confluence on 6-well dishes (Starstedt) or on Glass Bottom Petri Dishes (Willko) and transfected with Effectene reagent (Quiagen) according to the manufacturer's instructions.

All cell types were cultured at 37°C with 5% CO_2 in a humidified atmosphere.

3.*In vivo* fluorescence imaging

All imaging experiments were performed with the TCS SL laser scanning confocal microscope (Leica Microsystems) equipped with high numerical aperture objective (HCX PL Apo oil immersion 63X, 1.4 N.A.).

10^5 cells have been plated on Glass Bottom Petri Dishes (Wilko) and placed in the incubation chamber on the stage of the inverted microscope with controlled CO_2 (5%) and temperature (37°C).

An Argon laser was used for the excitation of CFP (excitation wavelength 458 nm) and YFP fluorophores (excitation wavelength 514 nm), while a He-Ne laser was used for the excitation of Alexa Fluor 633 (excitation wavelength 633nm).

4.Immunofluorescence

Cells were seeded on Glass Bottom Petri Dishes (Wilko) and after transfection were fixed with cold methanol for 5 min. Soon after fixation cells were permeabilyzed with 0.1% Triton X-100 and blocked for 30 min with the blocking solution (PBS+Tween 0,1% + BSA 1%- fresh). Primary antibody incubation has been done in blocking solution for 1h or O/N. Primary antibody used was: anti α-tubulin (Sigma-Aldrich), 1:1000, mouse. Excess antibody was eliminated by several washes with PBS 1X and secondary antibody incubation was performed in blocking solution for 1h.

Secondary antibody used was: Alexa Fluor anti mouse (Life Technologies), 1:200, goat. Glass Bottom Petri Dishes (Wilko) were mounted with Vectashield mounting media (Vector Laboratories).

5.FRET and FRAP experiments

For FRET experiments, the excitation and detection conditions of CFP and YFP fluorophores were set up. Typical parameters used for experiments are: 50% of 458nm laser intensity for CFP excitation and 10% of 514nm laser intensity for YFP excitation. The scanning rate is 400Hz and the zoom varies from a 4X to an 8X with a line average of 4-8. For sensitized emission FRET experiments three images of the same field of acquisition are required: the donor image (excitation of the donor and emission in the donor channel), the acceptor image (excitation of the acceptor and emission in the acceptor channel), the FRET image (excitation of the donor and emission in the acceptor channel).

Images have been acquired sequentially in order to minimize the cross talk between channels.

FRET analysis was performed by using two different plugins of the ImageJ software called Colocalization Analyzer and PixFRET (Feige et al., 2005; Hachet-Haas et al., 2006). The former plugin calculates the FRET index image starting from images acquired in the donor channel, in the acceptor channel and in the FRET channel. The first part of the plugin evaluates the Bleed Through Donor BT between the donor channel and the FRET channel, and Acceptor BT between the acceptor and the FRET channel. In our experimental conditions, the donor and the acceptor BT have a value respectively of 0.04 and 0.13. These parameters are used for the evaluation of the FRET index image defined as FRET index=$I_{FRET} - BT_{Donor} * I_{Donor} - BT_{Acceptor} * I_{Acceptor}$

The PixFRET plugin calculates a normalized FRET image and the FRET efficiency image. For normalized FRET images the plugin calculates the ratio between a FRET index images and the square root of the product between the donor and acceptor images: NFRET=(FRETindex/√I(donor)*I(acceptor)) *100.

FRET efficiency has been measured by Sensitized Emission, a method based on the evaluation of the variation in the acceptor emission intensity. FRET change is

observed when the distance or the orientation of the fluorophores varies, and so the resonance energy transfer from the donor to the acceptor.

In FRAP experiments images of cells expressing fluorescent proteins have been acquired with a scanning rate of 1000 Hz; even if this condition determines a reduced signal-to-noise ratio in the image, it allows faster acquisitions (656 ms for 512*512 images and 424 ms for 256*256 images). In the pre-bleaching condition, 10 images of a single cell have been acquired and 100-120 images after-bleaching to follow the recovery of the fluorescence intensity. 5 images of a circular ROI with an Area of 12.54um^2 at the maximum laser power were acquired during bleaching conditions.

The analysis of FRAP recovery curves involves both their correction for whole cell bleaching due to continuous irradiation and their normalization. Briefly, for the bleaching correction, the behavior in time of the fluorescence intensity of the whole cell was used to correct the recovery curve of the region of interest; this resulting curve was then normalized by dividing it for the mean of the fluorescence intensities of the ROI in the prebleach experiment. FRAP recovery curves have been fitted by a two phase exponential association function (OriginLab).

6.Western blot and antibodies

Transfected and not transfected cells were detached from plate using Trypsin 1X (Euroclone), washed with PBS and pelleted. Cells extracts were prepared in lysis buffer supplemented with protease and phosphatase inhibitors by lysis on ice for 30 minutes, and adding loading buffer 4x and denaturing at 100°C for 5 minutes. Membranes were blocked with 5% skimmed milk powder in TBS containing 0.1% Tween 20, and detection was carried out using specific primary antibodies. Primary antibodies for Western blot analyses were: TAU5 (Abcam), aa220-240, 1:1000, mouse; α-tubulin (Sigma-Aldrich), 1:5000, mouse; TAU46 aa404-441(Abcam), 1:200, mouse; Phospho-tau pSer262 1:250 (Thermo Scientific), rabbit; Phospho-tau pSer356 1.500 (Thermo Scientific), rabbit; GAPDH (Fitzgerald), 1:15000, mouse, actin(Sigma-Aldritch). Secondary antibodies HRP-conjugated anti-mouse or anti-rabbit or anti-goat were purchased by Santa Cruz Biotechnology, Inc. All the antibodies were diluted in 1% skimmed milk powder in TBS containing 0.1% Tween

20.

The signal detection has been made using ECL (Millipore) and Super Signal (Thermo Scientific) and acquired by ChemiDoc (Biorad).

7.Morphological analysis

Images for the morphological analysis were acquired as aforementioned in point 3. For the quantification of morphological parameters such as the total filament length and the number of branching points the filament tracer option of the IMARIS Bitplane software has been exploited. In detail, these two parameters are deduced by a software plugin that, based on connectivity and fluorescence intensity, automatically detects and segments filamentous structures revealing information about the topology of filaments as the sum of the lengths of all lines and the number of branching points within the filament.

RESULTS

1. CST-Q336H and CST-ΔK280 constructs have been generated by site-directed mutagenesis.

The plasmid containing the CST sequence has been subjected to site-directed mutagenesis. In order to isolate CST-Q336H and CST-ΔK280 mutated sequences, Dh5α cells have been transformed and plated on LB plates added with kanamycin. Twenty colonies have been picked and inoculated in LB medium. Each colony has been subjected to DNA extraction, and in order to screen positive colonies containing the CST-ΔK280 plasmid, a double digestion with restriction enzymes SacI and AgeI has been performed. The double digestion is expected to produce two DNA fragments of 4000kb and 2000kb (fig.1a; fig.1b). The same analysis has been performed for CST-Q336H mutant clones (data not show).

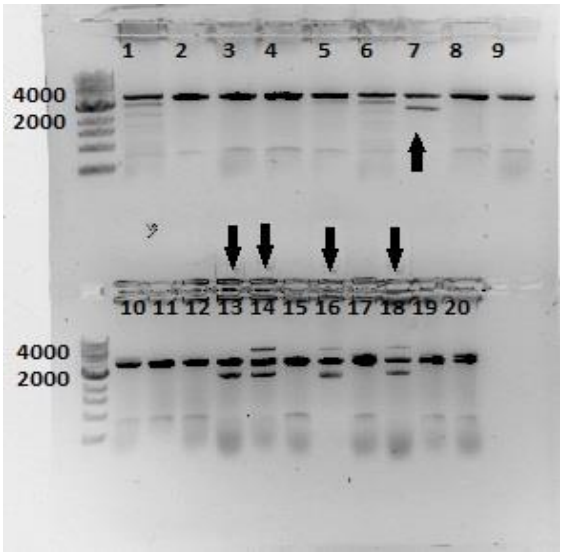

Figure 1a. Screening of positive clones carrying the ΔK280 mutation.

Candidate positive clones are: 7,13,14,16,18. Selected clones for subsequent analysis are indicated by black arrows.

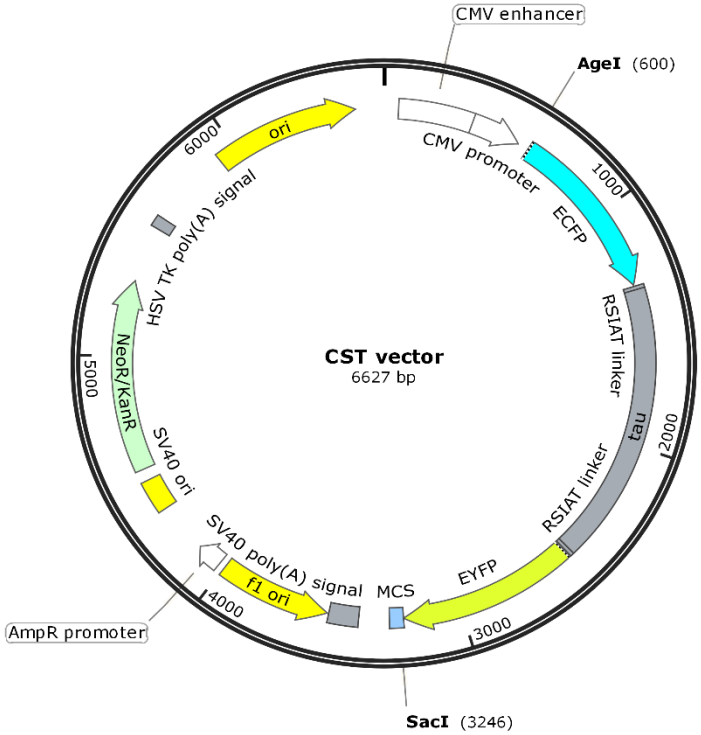

Figure 1b. CST vector map with SacI and AgeI sites.

Selected mutant clones have been subjected to DNA sequencing. The DNA sequences were analyzed with Snap Gene Viewer™ and Clustal Omega, to confirm the occurrence of the desired mutation. At the end of the screening one positive clone per each mutant has been selected.

2.CST-Q336H and CST- ΔK280 mutants binds to microtubules in living cells.

Hela cells have been transfected with the CST or CST-Q336H, CST-ΔK280 plasmid. After 24-48h, the expression of the exogenous proteins has been detected by live imaging at the confocal microscope. In order to perform a colocalization experiment with the CST and the microtubule network cells have been fixed and immunostained with anti α-tubulin antibodies and with a fluorescent secondary antibody emitting in the red channel. The sequential signal acquisition in the donor, acceptor and red channels, revealed that mutated CST (CST-Q336H and CST-ΔK280) colocalizes with tubulin (fig.2), indicating that they are able to interact with microtubules (MTs) as the CST.

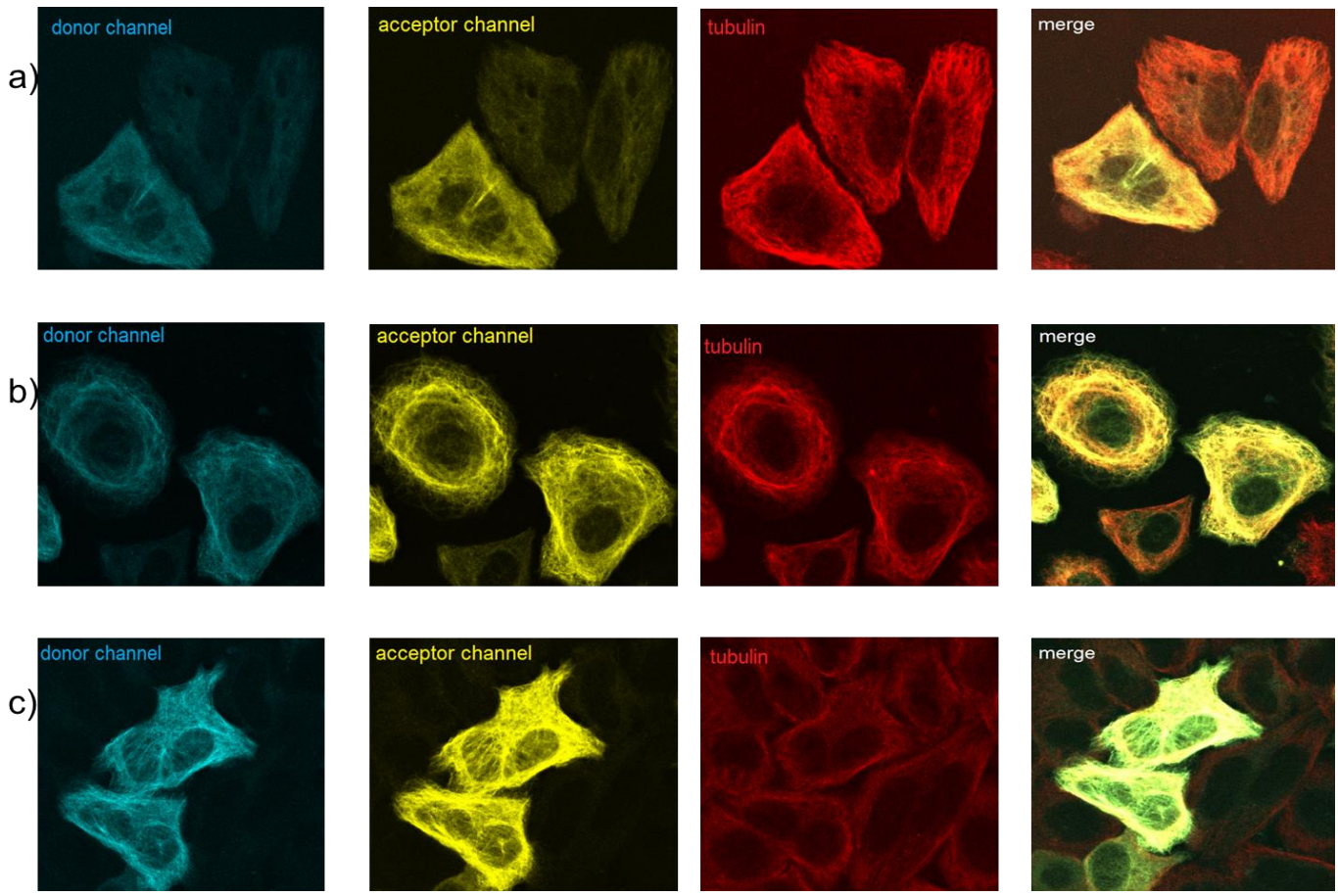

Fig.2. Expression of the CST in HeLa cells. Fluorescence signal of the CST (a) in the donor channel (blue), in the acceptor channel (yellow) and fluorescence signal of tubulin hybridized with anti α-tubulin antibody (red). Fluorescence signal of CST-Q336H (b), and CST- ΔK280 (c) in the donor channel (blue), in the acceptor channel (yellow) and of tubulin hybridized with the antibody anti α-tubulin (red).

3.CST-Q336H and CST-ΔK280 display different FRET signal efficiency compared to CST.

In order to analyze the changes in the protein conformation caused by the two mutation, HeLa cells expressing CST or CST-Q336H and CST-ΔK280 have been used to perform FRET experiments using the confocal microscope (fig.3).

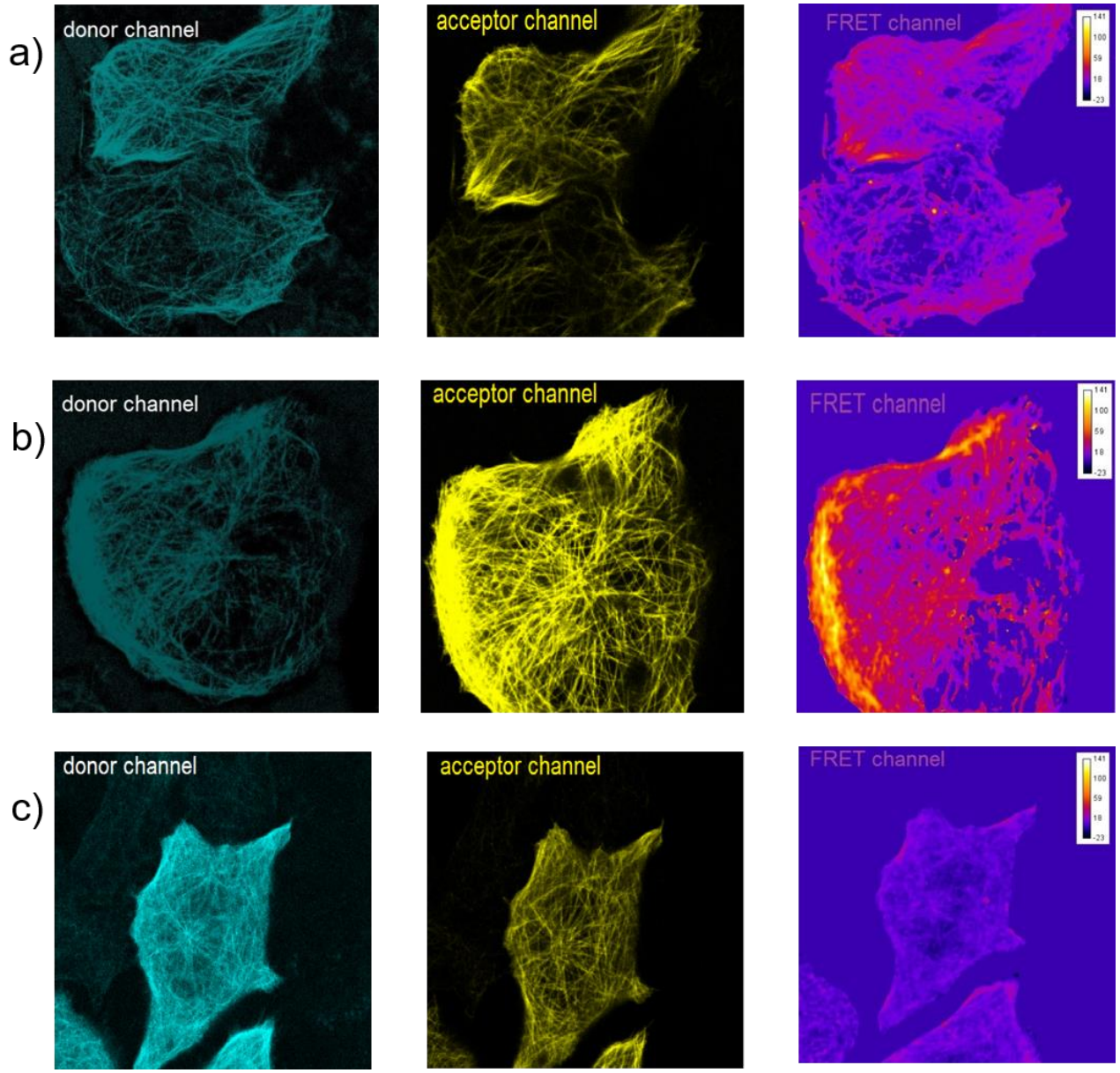

Figure 3. FRET detection in cell expressing CST and mutated sensors. Images of (a) CST, (b) CST-Q336H, (c) CST- ΔK280 acquired in the donor channel (blue), in the acceptor channel (yellow) and FRET channel. FRET index intensity is represented by a pseudocolor panel from dark blue to white indicating respectively the absence of FRET and the higher FRET.

The quantification and normalization of FRET values measured on fluorescent MTs have been performed employing the pixFRET plug in of the ImageJ software.

Normalized FRET values (NFRET) obtained for both mutated CST have been compared to the FRET efficiency of CST and reported in fig.4. FRET efficiency of CST was of 22.6, while CST-Q336H showed an increase in FRET efficiency (28.04). The CST-ΔK280 showed a significantly lower value (8.5), that cannot be considered a positive FRET signal at all. The increased FRET efficiency in the CST-Q336H suggest that the mutation induces a conformational change of Tau protein that reduces the distance between the donor and acceptor fluorophores, meaning that the N-terminal and the C-terminal are in closer contact than in wt Tau.

On the contrary, the very low FRET efficiency value obtained for CST-ΔK280 suggests an increase in the distance between CFP and YFP probably due to a more opened conformation of mutated Tau.

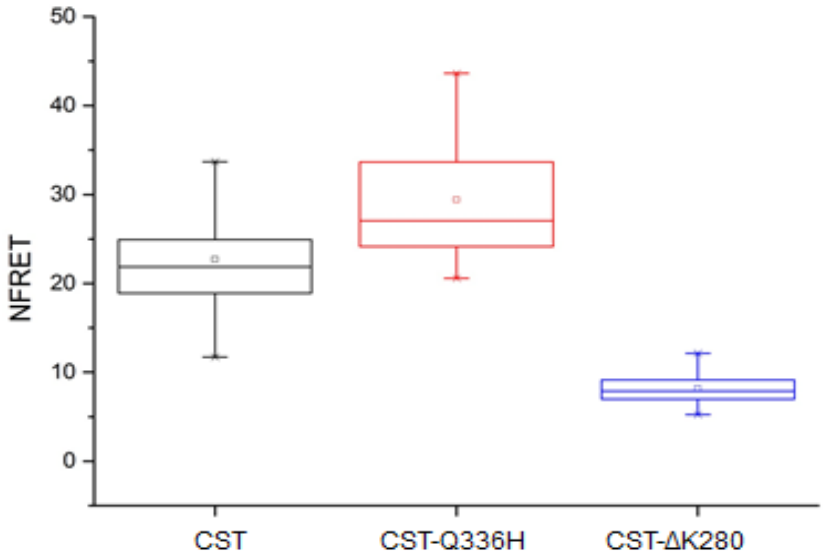

Figure 4. FRET analysis of wt and mutated CST sensors in living cells. The box plot reports normalized FRET values measured on fluorescent MTs in HeLa reporter cells. ANOVA One Way has been performed with a p-value threshold of 0.05. CST values are significantly different from CST-Q336H with a p-value of 0.00969, and from CST- ΔK280 with a p-value of 1.43835E-6. CST-Q336H and CST- ΔK280 differ significantly from each other with a p-value of 1.38779E-11.

4.CST- ΔK280, but not CST-Q336H mutation induced Tau protein cleavage in HeLa cells.

In order to study the role of Q336H and ΔK280 mutations in the context of CST, total protein extracts from cells expressing mutated CST have been analyzed by Western blot. For this analysis also the CST-AT8mut sample, carrying the S199A/S202A/T205A mutation that abolish phosphorylation at the AT8 epitope, has been included. Western blot results showed the CST full length at the expected molecular weight of 110kDa by hybridization with specific anti-Tau5, anti-Tau13 and anti-Tau46 antibodies which respectively recognize the central Tau portion, the 2-18 epitope and the 404-440 epitope of the longest tau isoform (fig.5). Other bands recognized at lower MW were detected represent CST fragments due to tau processing.

The fragment at 75kDa specifically detected by anti-Tau13 and anti-Tau46 antibodies is the result of a cleavage around the 404-440 epitopes, probably at the Asp421 which is the most prominent site of tau processing. Quantification of these results indicated that the CST- ΔK280 undergoes a more prominent cleavage than the other mutated constructs(fig.6).

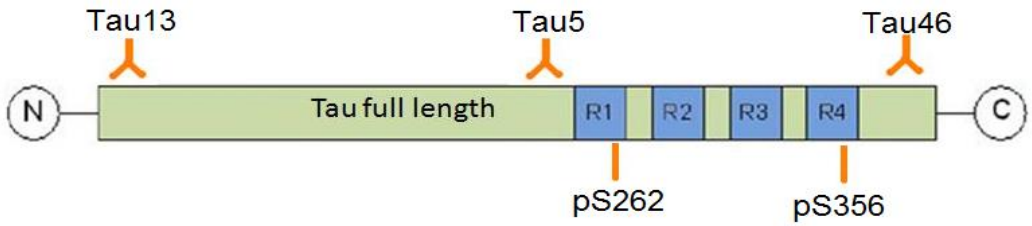

Figure 5. Antibodies specificity. Anti-Tau13 antibody targets the 2-18 epitope, anti-Tau5 antibody targets the 210-240 epitope, anti-Tau46 targets the 404-441 epitope. Anti-Ser262 Tau and Anti-Ser356 Tau are respectively targets respectively the first and the fourth repeat domain.

.

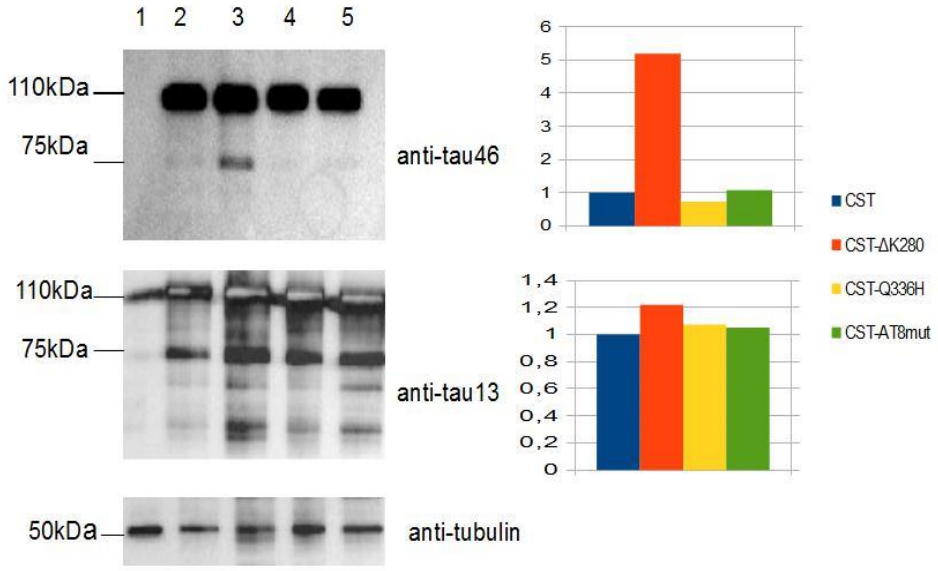

Figure 6. Western blot analysis of total protein extracts from wt and mutated CST expressing cells. Western blot lanes have been loaded as follows**:** 1)untransfected cells; 2)CST;3)CST-ΔK280;4)CST-Q336H;5)CST-At8mut.The full length exogenous proteins are indicated at 110kDa, anti-tubulin antibody has been used as loading control.

5.CST- ΔK280 is more phosphorylated at Ser262 and Ser356 with respect to CST in HeLa cells.

In order to analyze the phosphorylation profile of CST sensors, Western blot analysis of HeLa cells transfected with CST or with mutated constructs have been probed with anti-pS262 Tau antibody and ant-pS356 Tau antibody(fig.7).

Quantification with loading controls (gapdh and actin) confirmed that CST-ΔK280 is more phosphorylated than the other constructs both in Ser262 and Ser356 residues.

On the contrary, the CST is not phosphorylated in HeLa cells. The other mutated constructs appeared to be phosphorylated at different degrees. In particular, CST-Q336H and CST-ΔK280 appeared to be both significantly phosphorylated at Ser356.

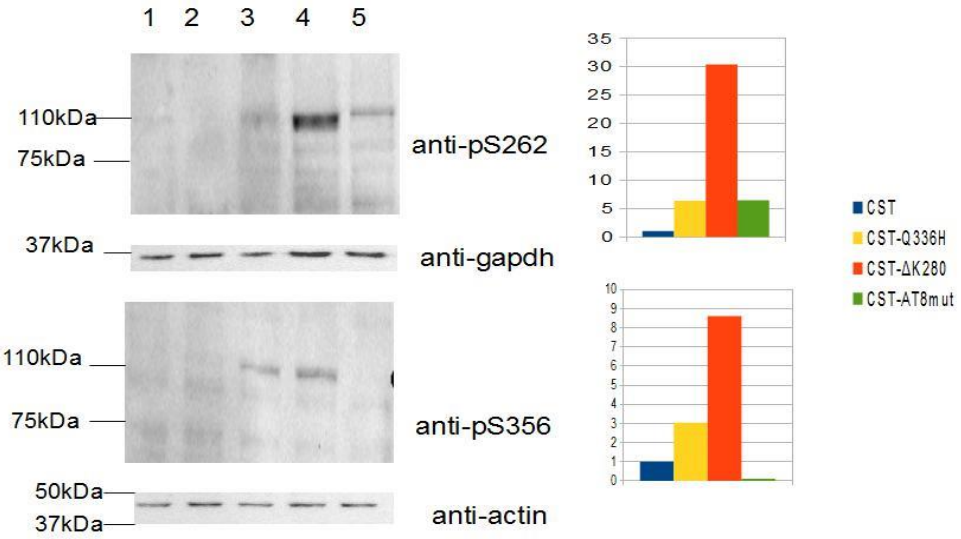

3

Figure 7. Phosphorylation profile by Western Blot analysis of HeLa cells transfected with the CST and the mutated CST constructs. Samples have been loaded as follows 1)untrasfected cells; 2)CST;3)CST-Q336H;4)CST-ΔK280;5)CST-At8mut.

6.Phosphorylation at pSer262 results to be the same in HT22 cells.

In order to analyze the phosphorylation profile of CST sensors in a more significant cell type, HT22 hippocampal immortalized neurons have been used.

Western blot analysis of HT22 cells transfected with CST or with mutated CST constructs have been probed with anti-pS262 Tau antibody (fig.8).

The result indicated that both the mutated constructs are phosphorylated, with CST-ΔK280 being more phosphorylated than CST-Q336H, as seen in HeLa cells. In addition, CST-AT8mut appeared to undergo a more prominent phosphorylation at that residue than the other constructs.

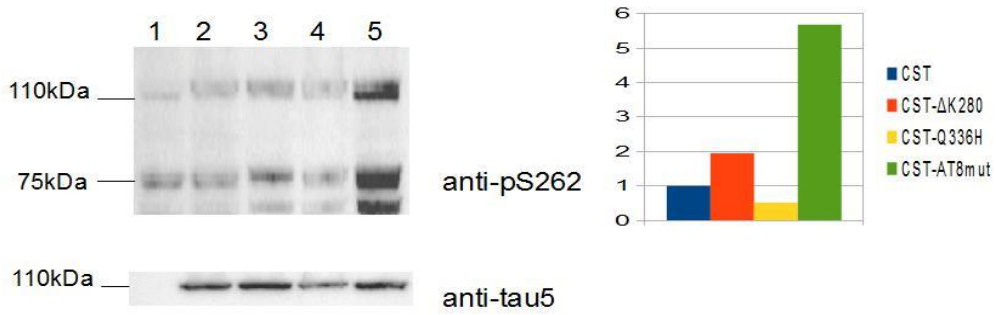

Figure 8. Phosphorylation profile by Western blot analysis of HT22 cells transfected with the CST and the other mutated constructs. The full length sensor at 110kDa is strongly phosphorylated in the CST-AT8mut lane than in the other mutated constructs. Samples have been loaded as follows 1)untransfected cells; 2)CST;3)CST-ΔK280;4)CST-Q336H;5)CST-At8mut.

7.ΔK280 and Q336H mutations displayed a different impact on Tau network complexity.

In order to study the impact of the two mutations on tau network complexity, an analysis of the morphological network complexity of tau has been carried out in HeLa cells expressing CST, CST-ΔK280 and CST-Q336H (fig.10). Images acquired by confocal microscopy have been subjected to image analysis by exploiting the IMARIS software that allow to collect two morphological parameters: the total filament length (that performs the summing of fluorescent filament segments) and the number of branching points (that calculates the number of crossing segments). Network complexity analysis indicated that ΔK280 mutation does not alter the total filament length and the number of branching points of Tau.

On the contrary the CST-Q336H analysis revealed an increase in both parameters. Indeed, this result indicated an increase in Tau network complexity due to Q336H mutation (fig.9).

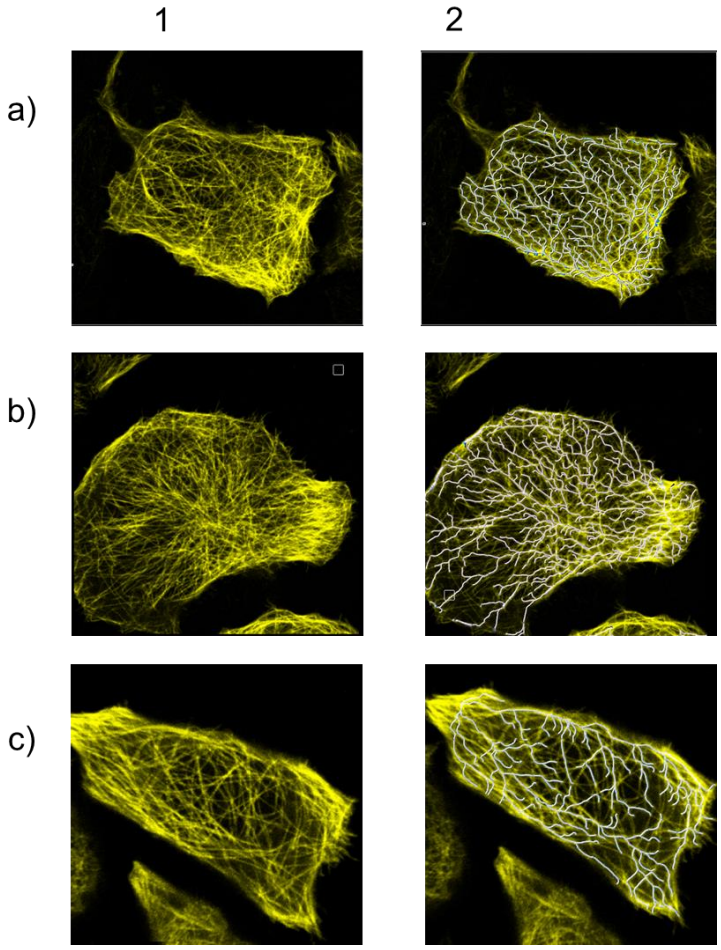

Figure 9. Morphological analysis of Tau network complexity in reporter HeLa cells expressing CST, CST-ΔK280 and CST-Q336H. Images taken before (1) and after (2) network analysis by IMARIS software.

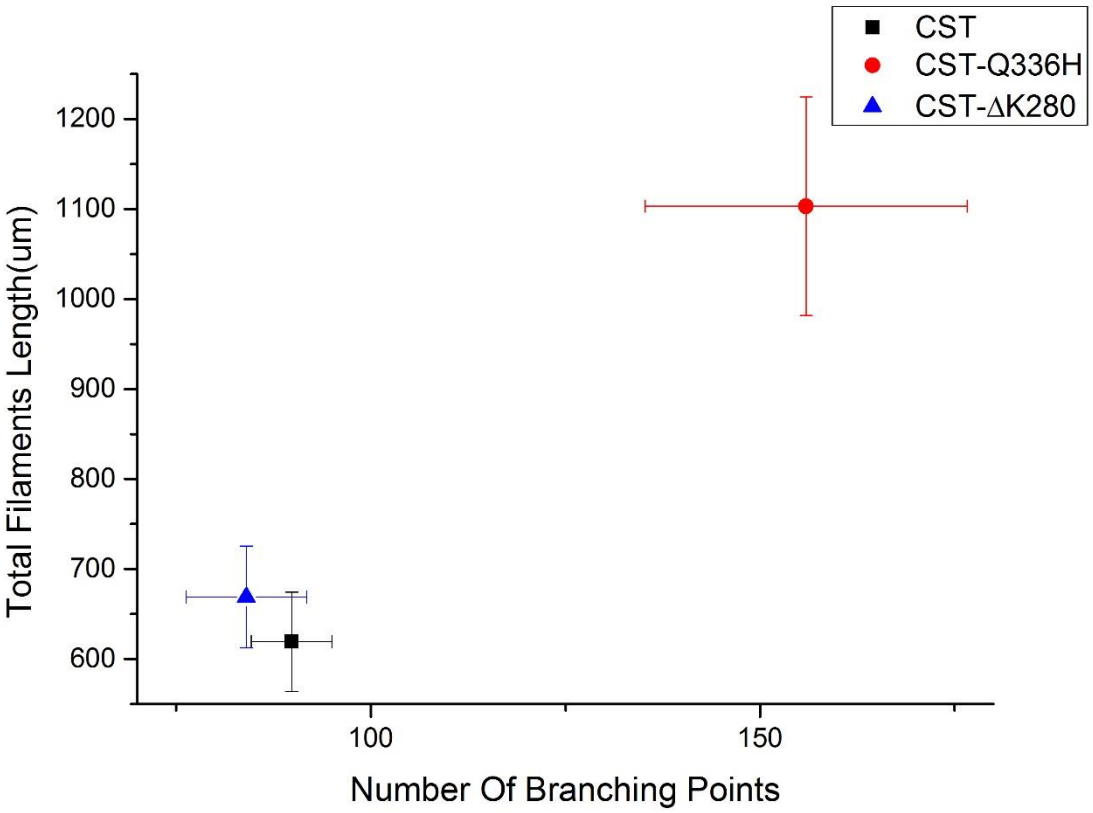

Figure 10. Analysis of Tau network complexity in cells expressing CST and mutated sensors. Images of (a) CST, (b) CST-Q336H, (c) CST- ΔK280 before (1) and after (2) network analysis by IMARIS software.

8.CST-ΔK280 has a higher mobility as revealed by FRAP analysis.

In order to analyze the involvement of the two mutations on tau mobility, FRAP analysis have been carried out in reporter cells expressing CST-Q336H, CST-ΔK280 and CST. A selected region of interest in the cells expressing the constructs was photo bleached and the recovery rate of the fluorescence intensity, due to the mobility of neighboring fluorescent molecules, was evaluated.

FRAP curves enabled to determine that 87% of CST molecules are in the mobile fraction, contributing to fill the bleached area. The recovery curve analysis revealed that two main components are represented in the mobile fraction: the 65% ascribed to a MTs binding phase that is characterized by a τ_1 of 30 sec and the 22% ascribed to diffusing soluble molecules with a τ_2 of 3,9 sec. Same analysis has been carried out for mutated constructs. The CST-Q336H displayed the same mobility as CST, indeed the 86% of molecules belong to the mobile fraction, with 64% in a MTs binding phase and a τ_1 of 31 sec, and the 22% assigned to diffusing soluble molecules with a τ_2 of 4,2 sec.

Differently, CST-ΔK280 displayed 90% of molecules in the mobile fraction, with 47% ascribed to a MTs binding phase that is characterized by a shorter time of recovery (τ_1 of 22 sec) and a remarkable increase in the diffusive fraction (43%) and a τ_2 of 2,7 sec (table 1; fig.11).

FRAP SAMPLE	MOBILE FRACTION(%)	FRACTION(%) AND TIME(sec)				STANDARD ERROR
CST	87	fract 1	65	τ_1	30,3	0,92
		fract 2	22	τ_2	3,9	0,2598
CST-Q336H	86	fract 1	64	τ_1	31,3	0,93
		fract 2	22	τ_2	4,22	0,25
CST-ΔK280	90	fract 1	47	τ_1	22,2	0,97
		fract 2	43	τ_2	2,7	0,14

Table 1. FRAP result of HeLa cells transfected with CST, CST-Q336H and CST-ΔK280. The table reports mobile fractions and times of recovery of HeLa cells transfected with indicated constructs.

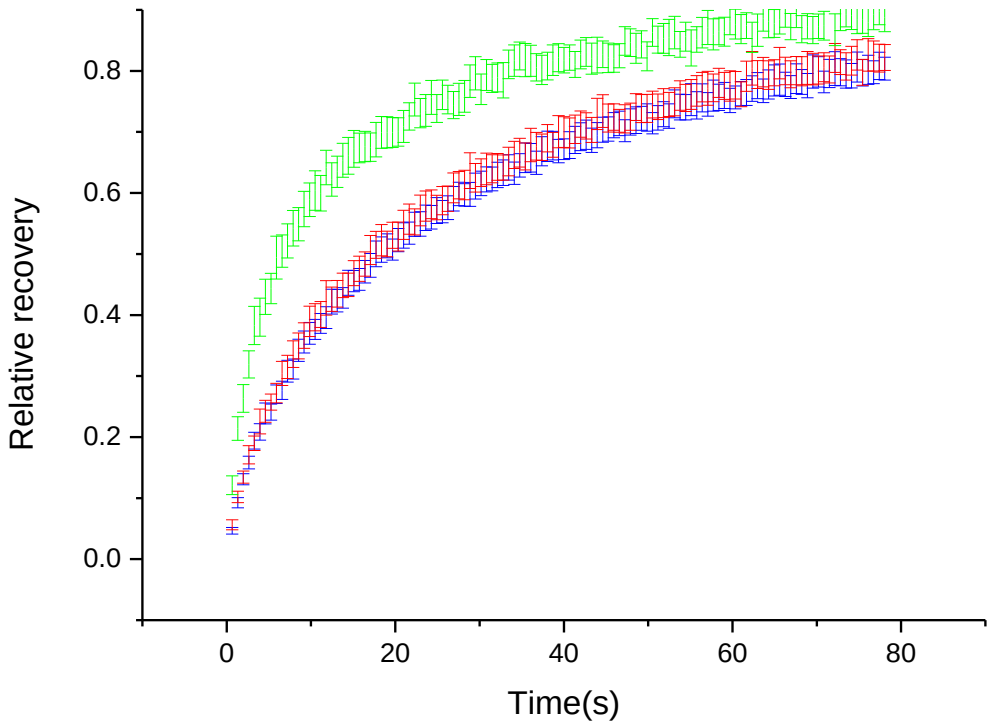

Figure 11. FRAP recovery curves of wt and mutated CST constructs. The blue and the red curves represents respectively the CST and the CST-Q336H, showing the same time of recovery. The green curve represents CST- ΔK280, with a faster time of recovery than the other two constructs.

DISCUSSION

1.Q336H and ΔK280 mutations impact at different extent tau conformational change.

Mutations in the MAPT locus that influence tau on a protein level have been observed to have an impact on its ability to bind to microtubules and in the regulation of their network.

The aim of this thesis is to avail the Conformational-Sensitive Tau Sensor (CST) to evaluate the role of Q336H and ΔK280 on protein conformation and its interaction with MTs. These two mutations, according to literature, have opposite effects on tau binding affinity of the protein to MTs. The first one, ΔK280, affects the gene on transcript and on protein level; in the first case inhibiting the insertion of the exon 10 causing a prevalence in the isoform 3R, in the second case reducing the interaction of tau with the MTs and its ability to regulate tubulin assembly. The second mutation, Q336H is a very rare mutation that has shown to increase the *in vitro* MTs rate assembly. Only two papers about the Q336H and Q336R mutations have been published and the *in vitro* study suggested a stronger binding affinity. ΔK280 mutation, on the contrary, has been extensively studied both *in vitro* and in transgenic animals. The CST displayed a positive FRET signal only when bound to MTs, while soluble molecules did not show a significant FRET signal. This demonstrated that the CST assumes a specific three-dimensional structure in which the C-terminal end approaches the N-terminal end so that the two fluorophores on the same molecule display a positive FRET. CST-Q336H showed a positive FRET signal too, but with a higher value, thus indicating that the mutated Tau bound the MTs assumed a conformation in which the two terminal ends are closer to each other. The increased proximity resulted in a more intense FRET signal.

Thus, our result confirms that, in the cellular context, this mutation has a role in the altered three-dimensional conformation of tau on MTs. In order to study the mobility of mutated CST, FRAP analysis have been performed. CST-Q336H resulted to have the same recovery curve as CST. This result showed that this mutation does not affect Tau binding to MTs. On the contrary, a recent study demonstrated that Q336H mutation increased Tau MTs binding affinity in *vitro* (Tacik *et al.*, 2015). Our

study demonstrated that, in the context of live cells, the Q336H mutation has a clear role in the three-dimensional conformation of tau, but is not involved in the regulation of MTs binding.

Moreover, tau/MTs interplay has been investigated by image analysis of fluorescent tau network: CST-Q336H showed a significant increase in network complexity, both in total filaments length and in number of branching points with respect to CST. The increased tau network complexity has to be further analyzed in order to investigate the complexity of the relative tubulin network.
CST-ΔK280 mutation showed a strong reduction of FRET signal, compared to CST, indicating that the deletion induced a conformational change in the protein that brings the two protein ends far from each other, at least at a distance > 50Å.
FRAP analysis demonstrated that the mobility of CST-ΔK280 is highly affected. Indeed the recovery curve indicated that tau molecules belonging to the MTs bound fraction are reduced (from 65 % to 47%) and conversely molecules ascribed to the diffusing soluble fraction increased (from 22% to 43%).Moreover, the time of recovery of both fractions is reduced suggesting that tau molecules could be partially cleaved. In addition, tau/MTs interplay has been investigated by image analysis of fluorescent tau network, and ΔK280 mutation resulted to not alter the total filament length and the number of branching points of Tau; further investigation of the complexity of the relative tubulin network has to be done.

2. Q336H and ΔK280 show different degree of phosphorylation at Ser262/Ser356.

Phosphorylation profile by Western Blot analysis revealed that both CST-Q336H and CST-ΔK280 shows positive tau phosphorylation at Ser262/Ser356 in the MT-binding repeats.
CST-ΔK280 resulted to be significantly phosphorylated, with a thirty fold increase with respect to CST-Q336H in the Ser262 residue, and an eight fold increase in the Ser356 residue. According to the literature (Biernat et al., 1993; Biernat and Mandelkow 1999; Liu et al., 2007) tau phosphorylation at Ser262/Ser356 residues induces tau detachment from MTs. This suggests that the decrease in MTs binding fraction (measured in FRAP experiments) induced by ΔK280 could be also

enhanced by phosphorylation at these residues.

CST-Q336H showed to be more phosphorylated at Ser262/Ser356 five and three fold more than CST, respectively. Considering that Q336H displayed the same mobility than CST, this suggest that phosphorylation at these residues is not really significant for Tau/MTs interplay. The phosphorylation profile of the two mutations must be further analyzed to fully assess its impact on tau physiological functions.

3. ΔK280 but not Q336H mutation induced Tau protein cleavage in HeLa cells.

Western blot results indicated that ΔK280 deletion induced a more prominent tau protein cleavage. It is well known that ΔK280 strongly promotes the aggregation of tau into paired-helical filaments (PHFs) because it enhanced the propensity of the protein to form β-structure (Barghorn *et al.,* 2000). Indeed, C-terminally truncated PHF-core tau has the ability to capture full length tau and to enable sequential cycles of binding, truncation and binding, at least *in vitro* (Flores-Rodriguez *et al.*, 2015). The observed result suggested that the pro-aggregation behavior of ΔK280 mutant could be enhanced also by tau truncation.

On the contrary, Q336H does not induce a prominent tau cleavage, but in patients bearing this mutation have been observed to be present aggregates forming Pick Bodies, intracytoplasmic inclusions typical of Pick's Disease (Pickering-Brown *et al.*, 2004; Tacik *et al.*, 2015), indicating that the aggregation process could be stimulated also by other mechanisms to be uncovered.

FUTURE DIRECTIONS

To fully confirm the characterization of the two mutations, a more extensive study of phosphorylated epitopes has to be performed. Moreover, Western Blot analysis probed with PHF-1 Tau antibody, which recognizes 396/404 epitopes, will be performed, as these sites located in the C-region are known in literature to increase MTs assembly activity (Cho and Andrews, 2003; Liu *et al.*, 2007).

In addition, the preliminary results obtained in this thesis will be further validated *in vivo*. Indeed, to study the role of these two mutations during the onset and the progression of tau pathology, *in vivo* experiments in zebrafish embryos will be performed. With transient and stable strategies mutated CST constructs (downstream to a neural specific promoter) will be expressed in the nervous system allowing to monitor Tau pathology onset and progression by evaluating Tau conformational changes at different stages.

BIBLIOGRAPHY

1. Adamec, E., Mohan, P., Vonsattel, J.P., Nixon, R.A., 2002. Calpain activation in neurodegenerative diseases: confocal immunofluorescence study with antibodies specifically recognizing the active form of calpain 2. *Acta Neuropathol.*104, 92–104.

2. Ahmed Z, Bigio EH, Budka H, *et al.* Globular glial tauopathies (GGT): consensus recommendations. *Acta Neuropathol*. 2013: 126: 537-44.

3. Al-Bassam, J.; Ozer, R.S.; Safer, D.; Halpain, S.; and Milligan, R.A. MAP2 and tau bind longitudinally along the outer ridges of microtubule protofilaments. *J. Cell Biol.* **2002**, *157*, 1187–1196.

4. Alonso AD, Di Clerico J, Li B, *et al.*Phosphoryation of tau at Thr212, Thr231, and Ser262 combined causes neurodegeneration.*J Biol Chem*. 2010; 285(40):30851-30860.

5. Alonso AD, Zaidi T, Novak M, Grundke-Iqbal I, Iqbal K. Hyperphosphorilation induces self-assembly of tau into tangles of paired-helical filaments/straight filaments. *Proc Nat Acad Sci U S A.* 2001; 98:6923-6928.

6. Arima K. Ultrastructural characteristics of tau filaments in tauopathies: immuno-electron microscopic demonstration of tau filaments in tauopathies. *Neuropathology*. **2006** Oct;26(5):475-83.

7. Avila J, Lucas JJ, Perez M, Hernandez F. Role of tau protein in both physiological and pathological conditions. *Physiol Rev.* 2004 Apr;84(2):361-84.

8. Baker M,Litvan I, Houlden H, Adamson J, *et al.* Association of an extended haplotype in the tau gene with progressive supranuclear palsy. *Human Molecular Genetics,* 1999, Vol. 8, No. 4 711–715.

9. Bancher, C., Grundke-Iqbal, I., Iqbal, K., Fried, V.A., Smith, H.T., Wisniewski, H.M.,1991. Abnormal phosphorylation of tau precedes ubiquitination in neurofibrillary pathology of Alzheimer disease. *Brain Res*. 539, 11–18.

10. Barghorn S, Zheng-Fishhöfer Q, Ackmann M *et al.*Structure, microtubule interactions, and paired helical filaments aggregation by tau mutants of frontotemporal dementias. *Biochemistry* 2000 Sep 26;39(38):11714-21.

11. Biernat J, Gustke N, Drewes G, *et al.*Phosphoryation of Ser262 strongly reduces binding of tau to microtubules: distinction between PHF-like immunoreactivity and microtubule binding. *Neuron* 1993; 11:153-163.

12. Biernat J, Mandelkow EM.The development of cell processes induced by tau proteins requires phosphorylation of serine 262 and 356 in the repeat domain and is inhibited by phosphorylation in the proline-rich domains. *Mol Biol Cell* 1999; 10:727-740.

13. Brandt R.; Léger, J.; Lee, G. Interaction of tau with the neural plasma membrane mediated by tau's amino-terminal projection domain. *J. Cell Biol.* **1995**, *131*, 1327–1340.

14. Breuzard G, Hubert P, Nouar R, et al. Molecular mechanisms of Tau binding to microtubules and its role in microtubule dynamics in live cells. *J Cell Sci.*2013;126(Pt 13):2810-2819.

15. Brunden KR, Trojanowski JQ, Lee VM. Evidence that non-fibrillar tau causes pathology linked to neurodegeneration and behavioral impairments. *J Alzheimers Dis* 2008; 14:393-9.

16. Bunker JM, Kamath K, Wilson L *et al.* FTDP-17 mutations compromise the ability of tau to regulate microtubule dynamics in cells. *J Biol Chem* 2006 Apr 28;281(17):11856-63.

17. Cardullo RA, Mungovan RM, Wolf DE. Imaging membrane organization and dynamics. In: Dewey G, editor. *Biophysical and biochemical aspects of fluorescence spectroscopy*. New York. Plenum Press.pp 231-260.

18. Carisey A, Stroud M, Tsang R *et al.* Fluorescence recovery after photobleaching. Methods Bio Mol 769:387-402.

19. Chung CW, Song YH, Kim IK, et al. Proapoptotic effects of tau cleavage product generated by caspase-3. *Neurobiol Dis.* 2001;8(1):162-172.

20. Clavaguera F, Akatsu H, Fraser G, *et al.* Brain homogenates from human tauopathies induce tau inclusions in mouse brain. *Proc Natl Acad Sci U S A.* 2013 Jun 4;110(23):9535-40.

21. Clegg, R. Förster resonance energy transfer-FRET: what is it, why do it, and how it's done. In Gadella, Theodorus WJ. FRET and FLIM Techniques. Laboratory Techniques in Biochemistry and Molecular Biology, Volume 33. Elsevier. pp.1-57.

22. Cohen TJ, Guo JL, Hurtado DE, *et al.*The acetylation of tau inhibits its function and promotes pathological tau aggregation. *Nat Commun* 2011; 2:252.

23. Corsetti, V., Amadoro, G., Gentile, A., Capsoni, S., Ciotti, M.T., Cencioni, M.T., Atlante, A., Canu, N., Rohn, T.T., Cattaneo, A., Calissano, P., 2008. Identification of a caspase-derived N-terminal tau fragment in cellular and animal Alzheimer's disease models. *Mol. Cell Neurosci.* 38, 381–392.

24. Cowan CM, Mudher A. Are tau aggregates toxic or protective in tauopathies? *Front Neurol* 2013;13.4-114.

25. Crowther RA, Goedert M. Abnormal tau-containing filaments in neurodegenerative diseases. *J. Struct. Biol.*2000 Jun;130(2-3):271-9.

26. Daly NL, Hoffmann R, Otvos L, Craik DJ. Role of phosphorylation in the conformation of tau peptides implicated in Alzheimer's disease. *Biochemistry.* 2000;39(30):9039-9046.

27. de Calignon A, Polydoro M, Suarez-Calvet M *et al.* Propagation of tau pathology in a model of early Alzheimer's disease. *Neuron* 73 685-697.

28. Delacourte A, Robitaille Y, Sergeant N, *et al.*Specific pathological tau protein variants characterize Pick's disease. *J Neuropathol Exp Neurol.* **1996** Feb;55(2):159-68.

29. Dickson DW. Pick's Disease: a modern approach. *Brain Pathol.* 1998; **8**:339-54.

30. Dixit, R.; Ross, J.L.; Goldman, Y.E.; Holzbaur, E.L. Differential regulation of dynein and kinesin motor proteins by tau. *Science* **2008**, *319*, 1086–1089.

31. Donlon TA, Harris P, Neve RL. Localization of microtubule-associated protein tau (MBTB1) to chromosome 17q21. *Cytogenet Cell Genet*. 46: 607, 1987.

32. Eckermann K, Mocanu MM, Khlistunova I *et al.* The beta-propensity of tau determines aggregation and synaptic loss in inducible mouse models of tauopathy. *J Biol Chem* 2007 Oct 26;282(43):31755-65.

33. Farias, G.A.; Muñoz, J.P.; Garrido, J.; Maccioni, R.B. Tubulin, actin, and tau protein interactions and the study of their macromolecular assemblies. *J. Cell. Biochem*. **2002**, *85*, 315–324.

34. Feany MB, Dickson DW. Widespread cytoscheletal pathology characterizes corticobasal degeneration. *Am J Pathol*. **1995** Jun;146(6):1388-96.

35. Feige JN, Sage D, Wahli W, Desvergne B, Gelman L. PixFRET, an ImageJ plug-in for FRET calculation that can accommodate variations in spectral bleed-throughs.*Microsc Res Tech.* 2005;68(1):51-58.

36. Ferrer, I.; Barrachina, M.; Puig, B.; Martínez de Lagrán, M.; Martí, E.; Avila, J.; Dierssen, M. Constitutive Dyrk1A is abnormally expressed in Alzheimer disease, Down syndrome, Pick disease, and related transgenic models. *Neurobiol. Dis.* **2005**, *20*, 392–400.

37. Ferrer, I.; Blanco, R.; Carmona, M.; Puig, B. Phosphorylated mitogen-activated protein kinase (MAPK/ERK-P), protein kinase of 38 kDa (p38-P), stress-activated protein kinase (SAPK/JNK-P), and calcium/calmodulin-dependent kinase II (CaM kinase II) are differentially expressed in tau deposits in neurons and glial cells in tauopathies. *J. Neural Transm*. **2001**, *108*, 1397–1415.

38. Fischer D., Mukrasch M.D., Biernat J., Bibow S., Blackledge M., Griesinger C., Mandelkow E., Zweckstetter M. Conformational changes specific for pseudophosphorylation at serine 262 selectively impair binding of tau to microtubules. *Biochemistry*.2009;48:10047–10055.

39. Flores-Rodriguez P, Ontiveros-Torres M, Cárdenas-Aguayo MC, *et al.*The relationship between truncation and phosphorylation at the C-terminus of tau protein in the paired-helical filaments of Alzheimer's disease. *Frontiers of Neuroscience* 9:33, February 2015.

40. Förstl H, Kurz A. Clinical features of Alzheimer's disease. *Eur Arch Psychiatry Clin Neurosci.* 1999;249(6):288-290.

41. Foster NL, Wilhelmsen K, Sima AAF, *et al.* Frontotemporal Dementia and Parkinsonism Linked to Chromosome 17: A Consensus Conference. *Ann. Neurol.* 1997; 41:706-715.

42. Frost B, Jacks RL, Diamond MI (2009). Propagation of the tau misfolding from the outside to the inside of a cell. *J Biol Chem* 284: 12845-12852.

43. Gamblin TC, Chen F, Zambrano A, Abraha A *et al.* Caspase cleavage of tau:linking amyloid and neurofibrillary tangles in Alzheimer's Disease. *Procl Nat Acad Sci U S A* 100,10032-10037.

44. Gao L, Tucker KL, Andreadis A. Transcriptional regulation of the mouse microtubule-associated protein tau. *Biochim Biophys Acta* 2005 Jan 11,1681(2-3):175-81.

45. Gasparini L, Terni B, Spillantini MG. Frontotemporal dementia with tau pathology. *Neurodegen Dis* 2007; 4:236-253.

46. Ghetti B, Oblak AL, Boeve BF, *et al.* Invited review: Frontotemporal dementia caused by microtubule-associated protein tau gene (MAPT) mutations: a chameleon for neuropathology and neuroimaging. *Neuropathology and Applied Neurobiology* (2015), **41**, 24–46.

47. Goedert M, Jakes R, Spillantini MG *et al.*Assembly of microtubule-associated protein tau into Alzheimer-like filaments induced by sulphated glycosaminoglycans. *Nature* 383(6600):550-3.

48. Goedert M, Wischik CM, Crowther RA *et al.*Cloning and sequencing of the cDNA encoding a core protein of the paired-helical filament of Alzheimer's Disease: identification as the microtubule-associated protein tau. *Proc Natl Acad Sci U S A.*1988 Jun;85(11):4051-55.

49. Goode BL, Feinstein S. Identification of a novel microtubule binding and assembly domain in the developmentally regulated inter-repeat region of tau. *The Journal of Cell Biology* 124(5):769-82.

50. Guillozert-Bongarts Al, Cahill ME, Cryns VL, *et al.*Pseudophosphorylation of tau at serine 422 inhibits caspase cleavage: in vitro evidence and implications for tangle formations in vivo. *J Neurochem*. 2006; 97(4):1005-1014.

51. Guillozet-Bongaarts AL, Garcia-Serra F, Reynolds MR *et al.*Tau truncation during neurofibrillary tangle evolution in Alzheimer's disease. *Neurobiol. Aging*. 2005 Jul;26(7):1015-22.

52. Hachet-Haas M, Converset N, Marchal O, et al. FRET and colocalization analyzer--a method to validate measurements of sensitized emission FRET acquired by confocal microscopy and available as an ImageJ Plug-in. *Microsc Res Tech.* 2006;69(12):941-956.

53. He, H.J.; Wang, X.S.; Pan, R.; Wang, D.L.; Liu, M.N.; He, R.Q. The proline-rich domain of tau plays a role in interactions with actin. *BMC Cell Biol*. **2009**, *10*, 81.

54. Heicklen-Klein *et al.*Tau promoter confers neuronal specificity and binds Sp1 and AP-2.*J.Neurochem* 2000 Oct, 75(4) 1408-18.

55. Hirokawa, N.; Shiomura, Y.; Okabe, S. Tau proteins: The molecular structure and mode of binding on microtubules. *J. Cell Biol.* **1988**, *107*, 1449–1459

56. Höglinger GU, Melhem NM, Dickson DW, *et al.*Identification of common variants influencing risk of the tauophaty progressive supranuclear palsy. *Nat.Genet.* 2011 Jun 19;43(7):699-705.

57. Holmes BB, Furman JL, Mahan TE *et al.* Proteopatic tau seeding predicts tauopathy in vivo. *Proc Nat Acad Sci U S A* 2014 111, E4376-E4385.

58. Horiguchi, T., Uryu, K., Giasson, B.I., Ischiropoulos, H., LightFoot, R., Bellmann, C., Richter-Landsberg, C., Lee, V.M., Trojanowski, J.Q., 2003. Nitration of tau protein is linked to neurodegeneration in tauopathies. *Am. J. Pathol.* 163, 1021–1031.

59. Houlden H, Baker M, Morris HR, *et al.* Corticobasal degeneration and progressive supranuclear palsy share a common tau haplotype. 2001 *Neurology* 56:1702–1706.

60. Hutton M, Lendon CL, Rizzu P *et al.* Association of missense and 5'-splice-site mutations in tau with the inherited dementia FTDP-17. *Nature* 1998 Jun 18, 393(6686):702-5.

61. Hyman BT, Augustinack JC, Ingelsson M. Transcriptional and conformational changes of the tau molecule in Alzheimer's disease. Biochim Biophys Acta 2005; 1739:150-157.

62. Iba M, Guo JL, McBride JD. Synthetic tau fibrils mediate transmission of neurofibrillary tangles in a transgenic mouse model of Alzheimer's disease-like tauopathy. *J Neurosci* 33:1024-1037 (2013).

63. Iqbal K *et al.*Protein changes in senile dementia. *Brain Res.* **77** 337-343 (1977).

64. Iqbal, K., Alonso, A.C., Gong, C.X., Khatoon, S., Pei, J.J., Wang, J.Z., Grundke-Iqbal, I.,1998. Mechanisms of neurofibrillary degeneration and the formation of neurofibrillary tangles. *J. Neural. Transm. Suppl*. 53, 169–180.

65. Irwin DJ, Cohen TJ, Grossman M, *et al.*Acetylated tau neuropathology in sporadic and hereditary tauopathies. *Am J Pathol* 2013 Aug;183(2):344-51.

66. Irwin DJ, Cohen TJ, Grossmann M, *et al.*Acetylated tau, a novel pathological signature in Alzheimer's disease and other tauopathies. *Brain* 2012; 135(Pt.3) 807-818.

67. Ittner, L.M.; Ke, Y.D.; Delerue, F.; Bi, M.; Gladbach, A.; van Eersel, J.; Wölfing, H.; Chieng, B.C.; Christie, M.J.; Napier, I.A.; *et al*. Dendritic function of tau mediates amyloid-beta toxicity in Alzheimer's disease mouse models. *Cell* **2010**, *142*, 387–397.

68. Jeganathan S, von Bergen M, Mandelkow EM, Mandelkow E. The natively unfolded character of tau and its aggregation to Alzheimer-like paired-helical filaments. *Biochemistry* 2008 Oct 7; 47(40):10526-39.

69. Jung, D.; Filliol, D.; Miehe, M.; Rendon, A. Interaction of brain mitochondria with microtubules reconstituted from brain tubulin and MAP2 or TAU. *Cell Motil. Cytoskeleton* **1993**, *24*, 245–255.

70. Karch CM, Goate AM. Alzheimer's Disease Risk Genes and Mechanisms of Disease Pathogenesis. *Biol Psychiatry.* 2014

71. Klein, C.; Kramer, E.M.; Cardine, A.M.; Schraven, B.; Brandt, R.; Trotter, J. Process outgrowth of oligodendrocytes is promoted by interaction of fyn kinase with the cytoskeletal protein tau. *J. Neurosci.* **2002**, *22*, 698–707.

72. Landino LM, Skreslet TE, Alston JA *et al.*Cysteine oxidation of tau and

microtubule-associated protein-2 by peroxynitrite: modulation of microtubule assembly kinetics by the thioredoxin reductase system. *J Biol Chem* 2004, 279, 35101-35105.

73. Ledesma MD, Medina M, Avila J. The in vitro formation of recombinant tau polymers: effect of phosphorylation and glycation. *Mol Chem Neuropathol* 27, 249-258.

74. Lee G, Neve RL, Kosik KS. The primary structure and heterogeneity of tau protein from mouse brain. *Science*, **239,** 285-88.

75. Lee, M.S.; Kwon, Y.T.; Li, M.; Peng, J.; Friedlander, R.M.; Tsai, L.H. Neurotoxicity induces cleavage of p35 to p25 by calpain. *Nature* **2000**, *405*, 360–364.

76. Leroy, K.; Boutajangout, A.; Authelet, M.; Woodgett, J.R.; Anderton, B.H.; Brion, J.P. The active form of glycogen synthase kinase-3β is associated with granulovacuolar degeneration in neurons in Alzheimers's disease. *Acta Neuropathol*. **2002**, *103*, 91–99.

77. Li, G.; Yin, H.; Kuret, J. Casein kinase 1 delta phosphorylates tau and disrupts its binding to microtubules. *J. Biol. Chem.* **2004**, *279*, 15938–15945.

78. Liu F, Li B, Tung EJ *et al.*Site-specific effects of tau phosphorylation on its microtubule assembly activity and self-aggregation. *Eur J Neurosci.* 2007 December; 26(12):3429-3436.

79. Liu F, Liang ZH, Shi JH, Yin DM *et al.*PKA modulates GSK-3β and cdk-5-catalyzed phosphorylation of tau in site-and kinase-specific manners. *FEBS lett* 2006; 580:6269-6274.

80. Liu L, Drouet V, Wu JW *et al.*Trans-synaptic spread of tau pathology in vivo.

PloS One 7:e31302.

81. Liu, Y.H., Wei, W., Yin, J., Liu, G.P., Wang, Q., Cao, F.Y., Wang, J.Z., 2009c. Proteasome inhibition increases tau accumulation independent of phosphorylation. *Neurobiol. Aging* 30, 1949–1961.

82. Lovestone S, Hartley CL, Pearce J, Anderton BH (1997). The phosphorylation of tau: a critical stage in neurodevelopmental and neurodegenerative processes. *Neuroscience* 78:309-324.

83. Luna-Munoz J, Chavez-Macias L, Garcia-Serra F, Mena R. Earliest stage of tau conformational changes are related to the appearance of a sequence of specific phospho-dependent tau epitopes in Alzheimer's Disease. *J Alzheimers Dis.* 2007 Dec;12(4):365-75.

84. Mandelkow EM, Mandelkow E. Biochemistry and cell biology of tau protein in neurofibrillary degeneration. *Cold Spring Harb.Perspect.Med*. 2012, 2, a006247.

85. Mena R, Luna-Munoz J. Stages of pathological tau-protein processing in Alzheimer's disease:from soluble aggregation to polymerization into insoluble tau-PHFs, in *Current Hypoteses and Research Milestones*, ed Maccioni RB, Perry G. editors (Busines) 79-91(2009).

86. Mena, R., Edwards, P.C., Harrington, C.R., Mukaetova-Ladinska, E.B., Wischik, C.M.,1996. Staging the pathological assembly of truncated tau protein into paired helical filaments in Alzheimer’s disease. Acta Neuropathol. 91, 633–641.

87. Mocanu MM, Nissen A, Eckermann K *et al.* The potential for beta-structure in the repeat domain of tau protein determines aggregation, synaptic decay, neuronal loss, and coassembly with endogenous tau in inducible mouse

models of tauopathy. *J Neurosci* 2008 Jan16;28(3):737-48.

88. Morris HR, Baker M, Yasojima K, *et al.* Analysis of tau haplotypes in Pick's Disease. *Neurology* August 13, 2002 Vol.59 no.3 443-445.

89. Mukrasch, M.D.; von Bergen, M.; Biernat, J.; Fischer, D.; Griesinger, C.; Mandelkow, E.; Zweckstetter, M. The “jaws” of the tau-microtubule interaction. *J. Biol. Chem.* **2007**, *282*, 12230–12239.

90. Mullineaux CW, Kirchhoff H. 2007 Using fluorescence recovery after photobleaching recovery interrogates entire cell surfaces. *Biophys* J 75:1131-1138.

91. Munoz DG, Ludwin SK. Classic and generalized variants of Pick's Disease: a clinicopathological, ultrastructural, and immunocytochemical comparative study. *Annals of neurology*. 1984; 16:467-480.

92. Munoz DG, Ros R, Fatas M, *et al.* Progressive nonfluent aphasia associated with a new mutation V363I in tau gene. *Am J Alzheimers Dis Other Dement.* 2007 Aug-Sep;22(4):294-9.

93. Murthy SN, Wilson JH, Lukas TJ *et al.* Cross-linking sites of the human tau protein, probed by reactions with human transglutaminase. *J Neurochem* 71, 2607-2614.

94. Nickel W, Rabouille C (2009) Mechanisms of regulated unconventional protein secretion. *Nat Rev Mol Cell Biol* 10:148-155.

95. Niewiadomska, G.; Baksalerska-Pazera, M.; Lenarcik, I.; Riedel, G.J, Compartmental protein expression of Tau, GSK-3beta and TrkA in cholinergic neurons of aged rats. *J. Neural Transm.* **2006**, *113*, 1733–1746.

96. Niewiadomska, G.; Baksalerska-Pazera, M.; Riedel, G. Altered cellular distribution of phospho-tau proteins coincides with impaired retrograde axonal transport in neurons of aged rats. *Ann. N. Y. Acad. Sci.* **2005**, *1048*, 287–295.

97. Nouar R, Devred F, Breuzard G, Peyrot V. FRET and FRAP imaging: approaches to characterise tau and stathmin interactions with microtubules in cells. *Biol Cell.*2013;105(4):149-161.

98. Oide T, Kinoshita T, Arima K(2006) Regression stage senile plaques in the natural course of Alzheimer's disease. *Neuropathol Appl Neurobiol* 32:539-556.

99. Olenych, S.G.; Claxton, N.S.; Ottenberg, G.K.; Davidson, M.W. The fluorescent protein color palette. *Curr Protoc Cell Biol.* **2007.**

100. Panda, D.; Samuel, J.C.; Massie, M.; Feinstein, S.C.; Wilson, L. Differential regulation of microtubule dynamics by three- and four-repeat tau: Implications for the onset of neurodegenerative disease. *Proc. Nat. Acad. Sci. USA* **2003**, *100*, 9548–9553.

101. Patrick, G.N.; Zukerberg, L.; Nikolic, M.; de la Monte, S.; Dikkes, P.; Tsai, L.H. Conversion of p35 to p25 deregulates Cdk5 activity and promotes neurodegeneration. *Nature* **1999**, *402*, 615–622.

102. Pei, J.J.; Tanaka, T.; Tung, Y.C.; Braak, E.; Iqbal, K.; Grundke-Iqbal, I. Distribution, levels, and activity of glycogen synthase kinase-3 in the Alzheimer disease brain. *J. Neuropathol. Exp. Neurol.* **1997**, *56*, 70–78.

103. Pevalova M, Filipcik P, Novak M, Avila J, Iqbal K. Post-translational modifications of tau protein. *Bratisl Lek Listy.* 2006;107(9-10):346-353.

104. Pickering-Brown SM, Baker M, Nonaka T *et al.*Frontotemporal dementia with Pick-type histology associated with Q336R mutation in the tau gene. *Brain*

2004 Jun;127(Pt.6):1415-26.

105. Pittmann AM, Myers AJ, Duckworth J, Bryden L *et al.*The structure of the tau haplotype in controls and in progressive sopranuclear palsy. *Hum. Mol. Genet.*13: 1267-1274, 2004.

106. Plouffe V, Nguyen-Vi M, Rivest-McGraw J *et al*.Hyperphosphorilation and cleavage at D421 Enhance Tau Secretion (2012) PloS One 7(5):e36873

107. Ponnanbalam S(2003) Protein secretion and the Golgi apparatus. *Mol Membr Biol* 20:97-98.

108. Recuero M, Serrano E, Bullido MJ, Valdivieso F (2004) Abeta production as consequence of cellular death of a human neuroblastoma overexpressing. *APP. FEBS. Lett* 3:114-118.

109. Reynolds, M.R., Reyes, J.F., Fu, Y., Bigio, E.H., Guillozet-Bongaarts, A.L., Berry,R.W., Binder, L.I., 2006b. Tau nitration occurs at tyrosine 29 in the fibrillar lesions of Alzheimer's disease and other tauopathies. *J. Neurosci.* 26, 10636–10645.

110. Rhein V, Eckert A (2007) Effects of Alzheimer's amyloid-beta and tau protein on mitochondrial function-role of glucose metabolism and insulin signalling. *Arch Physiol Biochem* 113:131-141.

111. Rizzu P, Van Swieten JC, Joose M *et al*. High prevalence of mutations in the microtubule-associated protein tau in a population study of frontotemporal dementia in the Netherlands. *Am J Hum Genet* 1999 Feb 64(2) :414-21.

112. Rubinzstein DC. The role of intracellular protein-degradation pathways in neurodegeneration. *Nature* 443, 780-786.

113. Sergeant N, Bretteville A, Hamdane M *et al.*Biochemistry of Tau in Alzheimer's Disease and related neurological disorders. *Expert Rev Proteomics* 2008 Apr;5(2):207-24.

114. Shahpasand K, Uemura I, Saito T, *et al.*Regulation of mitochondrial transport and inter-microtubule spacing by tau phosphorylation at the sites hyperphosphorilated in Alzheimer's disease.J Neurosci. 2012;32(7):2430-2441.

115. Sharma, V.M.; Litersky, J.M.; Bhaskar, K.; Lee, G. Tau impacts on growth-factor-stimulated actin remodeling. *J. Cell Sci.* **2007**, *120*, 748–757.

116. Shimomura O. Discovery of green fluorescent protein (GFP) (Nobel Lecture).*Angew Chem Int Ed Engl* 2009 ;48(31)5590-602.

117. Singer, S.M., Zainelli, G.M., Norlund, M.A., Lee, J.M., Muma, N.A., 2002. Transglutaminase bonds in neurofibrillary tangles and paired helical filament tau early in Alzheimer's disease. *Neurochem. Int*. 40, 17–30.

118. Smett-Nocca C, Broncel M, Wieruszeski JM, *et al.*identification of O-GlcNAc sites within peptides of the Tau protein and their impact on phosphorylation. *Mol BioSyst*. 2011, 7, 1420-1429.

119. Spillantini MG, Crowther RA, Kamphorst W *et al.*Tau pathology in two Dutch families with mutations in the microtubule-binding region of tau. *Am J Pathol* 1998; 153:1359-63.

120. Spires-Jones TL, Kopeikina KJ, Koffie RM *et al.*Are tangles as toxic as they look? *J Mol Neurosci.*2011;45:438-44.

121. Stefansson H, Helgason A, Thorleifsson G, *et al.* A common inversion under selection in Europeans. *Nat. Genet.* 2005 Feb;37(2):129-37.

122. Steiner B,Mandelkow EM, Biernat J *et al.*Phosphoryation of microtubule-associated protein tau: identification of the site for Ca2+-calmodulin dependent kinase and relationship with tau phosphorylation in Alzheimer tangles.*EMBO J* 9:3539-3544.

123. Su B, Wang X, Lee HG *et al.*Chronic oxidative stress causes increased tau phosphorylation in M17 neuroblastoma cells. Neurosci. Lett. 2010,468, 267-271.

124. Tacik P, De Ture M, Lin WL, *et al.* A novel tau mutation, p.K317N, causes globular glial tauopathy. *Acta Neuropathol* 2015: Aug;130(2):199-214.

125. Tacik P, DeTure M, Hinkle KM *et al.*A novel tau mutation in Exon 12, p.Q336H, causes hereditary Pick's Disease. *J Neuropathol Exp Neurol* 2015.Nov;74 (11):1042-52.

126. Takahashi T, Mihara H. FRET detection of amyloid β-peptide oligomerization using a fluorescent protein probe presenting a pseudo-amyloid structure. *Chem Commun (Camb).* 2012;48(10):1568-1570.

127. Taniguchi-Watanabe S, Arai T, Kametani F, *et al.*Biochemical classification of tauopathies by immunoblot, protein sequence and mass spectrometric analyses of sarkosyl-insoluble and trypsin-resistant tau. *Acta Neuropatologica* (2016) 131:267–280.

128. Tolnay M, Clavaguera F. Argyrophilic grain disease: a late-onset dementia with distinctive features among tauopathies. *Neuropathology*, 2004; **24**:269-83.

129. Trinczek B, Biernat J, Baumann K *et al.*Domains of tau protein, differential phosphorylation, and dynamic instability of microtubules. *Mol Biol Cell.* 1995 Dec;6(12):1887-902.

130. Trinczek B, Biernat J, Baumann K, *et al.* Domains of tau protein, differential phosphorylation, and dynamic instability of microtubules.*Bio Mol Cell* 1995 Dec;6(12):1887-902.

131. van der Zee J, Van Broeckhoven C, Dementia in 2013:frontotemporal lobar degeneration-building on breakthroughs. *Nat Rev Neurol* 2014;**10**:70-2.

132. von Bergen M, Friedhoff P, Biernat J *et al.* Assembly of τ protein into Alzheimer paired-helical filaments depends on a local sequence motif (^{306}VQJVYK^{311}) forming β structure. *Proc Nat Acad Sci U S A.* 2000:97:5129-34.

133. Waters JC 2007.Live-cell fluorescence imaging.*Methods Cell Biol* 81:115-140.

134. Weingarten MD, Lockwood AH, Hwo SY, Kirschner MW. A protein factor essential for microtubule assembly. *Proc Natl Acad Sci U S A* 1975;72(5):1858-1862.

135. Weingarten, M.D.; Lockwood, A.H.; Hwo, S.Y.; Kirschner, M.W. A protein factor essential for microtubule assembly. *Proc. Natl. Acad. Sci. USA* **1975**, *72*, 1858–1862.

136. Wischik CM,Edwards PC, Lai RY *et al.* Selective inhibition of Alzheimer disease-like tau aggregation by phenothiazines. *Procl Nat Acad Sci U S A.* 93, 11213-11218.

137. Yamaguchi, H.; Ishiguro, K.; Uchida, T.; Takashima, A.; Lemere, C.A.; Imahori, K. Preferential labeling of Alzheimer neurofibrillary tangles with antisera for tau protein kinase (TPK) I/glycogen synthase kinase-3 beta and cyclin-dependent kinase 5, a component of TPK II. *Acta Neuropathol.* **1996**, *92*, 232–241.

138. Yu, J.Z.; Rasenick, M.M. Tau associates with actin in differentiating PC12 cells. *FASEB J.* **2006**, *20*, 1452–1461.

139. Yuzwa SA, Macauley MS, Heinonen JE *et al.*A potent mechanism inspired O-GlcNAcase inhibitor that blocks phosphorylation of tau in vivo. *Nat Chem Biol* 2008 4, 483-490.

140. Zhang YJ, Xu YF, Liu XH *et al.*Peroxynitrite induces Alzheimer-like tau modifications and accumulation in rat brain and its underlying mechanisms. *FASEB J* 2006, 20, 1431-1442.

141. Zhang, Y.J., Xu, Y.F., Chen, X.Q., Wang, X.C., Wang, J.Z., 2005b. Nitration and oligomerization of tau induced by peroxynitrite inhibit its microtubule-binding activity. *FEBS Lett.* 579, 2421–2427.